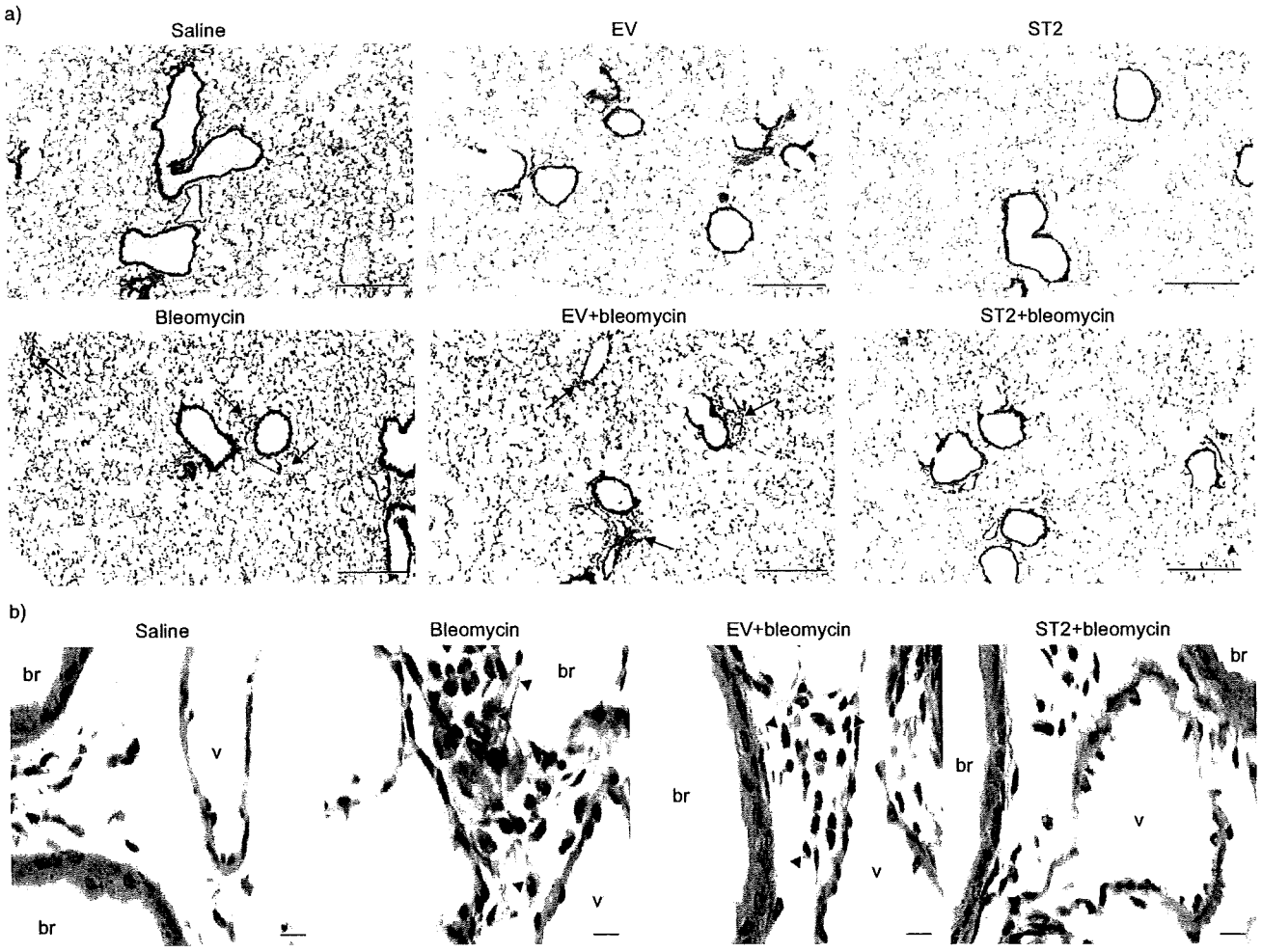

FIGURE 7. Histological findings at day 1 after treatment with bleomycin. Photomicrographs of lung sections from mice treated with saline, empty vector (EV; pCAGGS) alone, ST2 (pCAGGS-mST2) alone, bleomycin alone, EV plus bleomycin and ST2 plus bleomycin at day 1 after treatment. a) Lower magnification (Scale bars=200 μm) and b) focused on bronchovascular bundles at a higher magnification (Scale bars=10 μm) of mice treated with saline, bleomycin alone, EV plus bleomycin and ST2 plus bleomycin. Sections were stained with haematoxylin and eosin. Arrows: accumulation of inflammatory cells; arrowheads: neutrophils. br: bronchiole; v: vessel.

In order to examine the effect of the ST2 protein in mice, we first purified and administered recombinant ST2 protein to mice. However, unlike *in vitro* studies, an enormous amount of ST2 protein was needed in order to attain the high ST2 level *in vivo*. Then, a hydrodynamic injection method was employed, which is an efficient method for transient gene transfer to adult animals [13, 14, 19], and high levels of target gene expression can be achieved by the rapid injection of naked plasmid in a large volume. Corroborating previous reports [19], we confirmed that the main transgene-expressing organ was the liver; however, the ST2 protein was released into the systemic circulation and attained a high level 12 h after the gene transfer. The transgene expression level depends on the injection speed, injection volume, target organ and the choice of promoter of the plasmid vectors. We used the pCAGGS vector, which was driven by the chicken β-actin promoter that enabled us to maintain a high level of expression in mammalian cells. However, the appropriate plasma ST2 level to achieve an anti-inflammatory effect for mice treated with bleomycin has not been established *in vivo*. According to a previous report, 100 μg of ST2 protein is required to prevent endotoxin shock in mice [9]. Therefore, in the present study, we used a high dose of plasmid (50 $\mu g \cdot mouse^{-1}$) to obtain the maximal plasma concentration of ST2 (18.1–27.6 $\mu g \cdot mL^{-1}$).

In the present report, we demonstrated that the ST2 protein hindered the invasion of neutrophils and the subsequent capillary leakage in acute lung injury for the first time. In addition, TNF-α, IL-1β and IL-6 are known to play pivotal roles in the induction of lung inflammation, leukocyte migration, and the production of other cytokines and chemokines [20, 21], and these cytokines were elevated in BALF in bleomycin-induced acute lung injury. However, we found that the levels of TNF-α and IL-6 in BALF were significantly decreased in ST2-overexpressing mice at day 1 after bleomycin treatment. In previous *in vitro* experiments, it was demonstrated that ST2 inhibited the production of pro-inflammatory cytokines in macrophages derived from bone marrow [9, 11], as well as in a

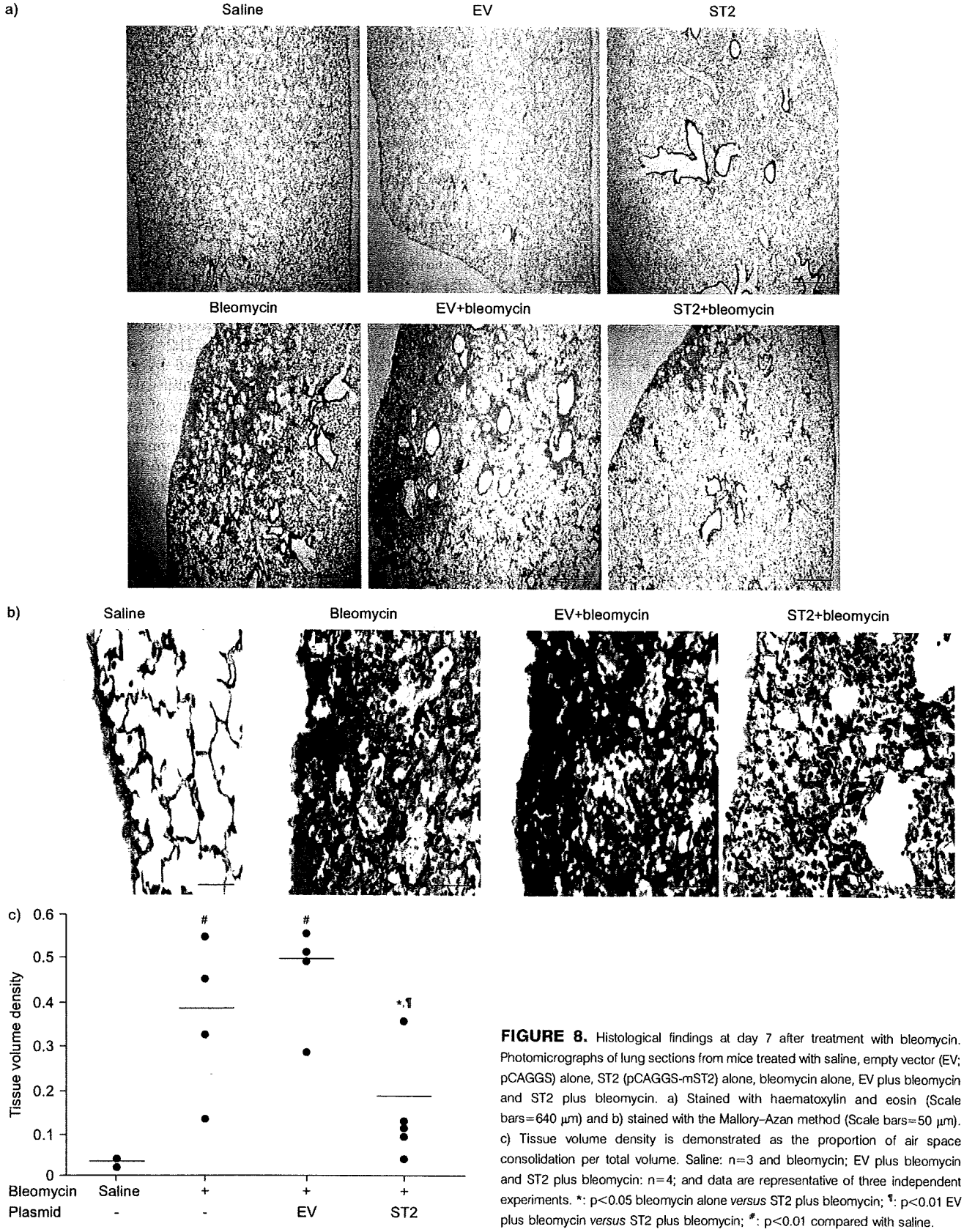

FIGURE 8. Histological findings at day 7 after treatment with bleomycin. Photomicrographs of lung sections from mice treated with saline, empty vector (EV; pCAGGS) alone, ST2 (pCAGGS-mST2) alone, bleomycin alone, EV plus bleomycin and ST2 plus bleomycin. a) Stained with haematoxylin and eosin (Scale bars=640 μm) and b) stained with the Mallory–Azan method (Scale bars=50 μm). c) Tissue volume density is demonstrated as the proportion of air space consolidation per total volume. Saline: n=3 and bleomycin; EV plus bleomycin and ST2 plus bleomycin: n=4; and data are representative of three independent experiments. *: $p<0.05$ bleomycin alone *versus* ST2 plus bleomycin; ¶: $p<0.01$ EV plus bleomycin *versus* ST2 plus bleomycin; #: $p<0.01$ compared with saline.

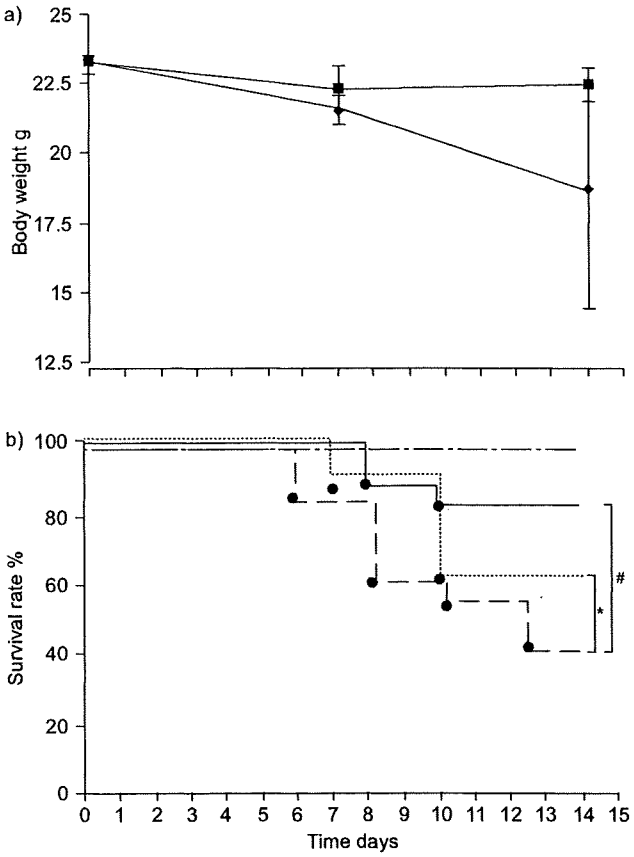

FIGURE 9. Body weight loss and survival rate of mice with bleomycin-induced lung injury. a) Comparison of body weight loss in mice treated with empty vector (EV) plus bleomycin (◆) and ST2 (pCAGGS-mST2) plus bleomycin (■) between day 0–14 (n=8 in both groups); p=0.08. b) The survival rate of mice was monitored for 14 days and analysed using the Kaplan–Meier method. Mice that died through injurious tracheotomy or deep anaesthesia were excluded. Saline (– · – · –): n=7; bleomycin alone (· · · ·): n=14; and EV plus bleomycin (- - - -) or ST2 plus bleomycin (——): n=23. *: p<0.05 bleomycin alone *versus* ST2 plus bleomycin; #: p<0.01 EV plus bleomycin *versus* ST2 plus bleomycin (see online supplementary material). Serum ST2 level after the injection of lipopolysaccharide (LPS) at 7.5 mg·kg^{-1} intravenously. This model mimicked human septic shock. The concentration of serum ST2 was examined using the mouse ST2 ELISA system. Serum ST2 were markedly elevated 12–24 h after LPS injection and rapidly declined at 48 h.

monocytic leukaemia cell line [10]. Therefore, in the present *in vivo* models, we speculated that overexpressed plasma ST2 infiltrated the alveolar spaces, where it affected alveolar macrophages to suppress the production of cytokines, and subsequently suppressed the migration of neutrophils and increased vascular permeability.

In contrast, we did not detect any significant differences in BALF findings from day 3 after bleomycin treatment. It was speculated that the following aetiological explanations might account for the BALF findings from day 3: 1) ST2 could play an anti-inflammatory role only during the initial phase of the acute lung injury, and thus, could not stop the infiltration of inflammatory cells after 3 days; 2) ST2 overexpression in this system peaked at 12–24 h after gene transfer, and then ST2 rapidly declined (thus, the effects of ST2 would diminish along with attenuation of the plasma concentration of ST2); and 3) ST2 could cause adverse effects from day 3 after bleomycin treatment. In association with the second point, hydrodynamic gene transfer is certainly an invasive approach; and thus, repetitive transfer was difficult in our pilot study, because the mice were often dead by repeated injection. Therefore, a method for maintaining high ST2 levels even after 48 h of gene transfer must be developed to assess the effects of ST2 accurately in this model. In association with the third point, it was reported that serum ST2 was elevated in some autoimmune diseases [22], and ST2L has been reported to play an important role in the differentiation of T-helper (Th) cells, which induce the proliferation and activation of Th2 response [22, 23]. Furthermore, a recent study reported that recombinant ST2 boosted hepatic Th2 responses *in vivo*, increased Th2 cytokines and advanced liver fibrosis [24]. It suggests that ST2 protein plays an ambivalent dual role as follows: ST2 suppresses the production of pro-inflammatory cytokines from macrophages (anti-inflammatory effect), and conversely, ST2 stimulates the Th2 response (pro-inflammatory effect). Considering these reports, we hypothesised that overexpresssed-ST2 protein may affect lymphocyte proliferation in this model, which would cause the adverse effects from the increase of total cells seen after day 3.

We found that endogenous ST2 mRNA and IL-33 were concurrently increased at day 3 after bleomycin treatment, whereas pro-inflammatory cytokines (TNF-α and IL-1β) were increased immediately after bleomycin treatment. The effects of ST2 and IL-33 have been well investigated in allergic diseases; IL-33 is known to strongly induce the production of Th2 cytokines and IgE and increase the proliferation of eosinophils [6, 25]. TAJIMA *et al.* [8] reported that endogenous ST2 and Th2 cytokines (IL-4, IL-5) were slowly induced after bleomycin-treatment, similarly to our study. From these results, endogenous ST2, Th2 cytokines and IL-33 would affect the progress of lung injury following the initial phase of acute lung injury. It is thought to be important whether overexpressed-ST2 affects IL-33 production; however, we could not approach that problem because of the difficulty of keeping the high level of ST2 at day 3 after bleomycin treatment.

From day 7 after bleomycin treatment, pulmonary remodelling progressed, and we found subpleural collapse and an increase of collagen fibres rather than peribronchial accumulation of inflammatory cells. Around half of the bleomycin-treated mice and half of the mice treated with empty vector plus bleomycin died during days 7–14, suggesting that the pulmonary remodelling phase (days 7–14) was most responsible for mortality. In ST2-overexpressing mice, the histological findings and survival rate after bleomycin treatment were improved compared with other bleomycin-treated mice. Pulmonary remodelling was mostly caused by the degradation of extracellular matrix by neutrophils [26] and the initial increase of neutrophils plays a critical role in the progress of lung inflammation and fibrosis [27]. Considering the previous reports and our present data, we found that inhibiting the infiltration of neutrophils by ST2 at an early stage of lung

injury helped to protect against proteolysis, minimised histological change and improved survival rates, even though the peribronchial inflammation, as indicated by the BALF findings, could not be completely suppressed.

In order to conclusively determine the roles of ST2, it will be necessary to conduct similar experiments using ST2 knockout (KO) mice. Although several studies using ST2 KO mice have been reported, unfortunately both specific soluble ST2 and transmembrane ST2L were absent in these mice, because the disrupted DNA of KO mice corresponds to a common portion of ST2 and ST2L [28]. Therefore, utilising available KO mice for the study of the involvement of ST2 in the lung inflammation would complicate the outcome. However, we speculate that previous results and the findings of the current study suggest that bleomycin would cause serious damage to the ST2-specific KO mice.

In conclusion, the present study confirmed that ST2 possesses the ability to suppress lung inflammation by inhibiting the elevation of pro-inflammatory cytokine levels and the accumulation of neutrophils, and by reducing vascular permeability. Further investigation into the aetiology of the effects of ST2 is required before the clinical applications are confirmed. However, ST2 could be a new candidate for the treatment of lethal acute lung injury.

ACKNOWLEDGEMENTS

The current authors would like to thank J. Miyazaki (Osaka University, Osaka, Japan) and T. Murakami (Jichi Medical Unfiversity, Tochigi, Japan) for providing plasmids and T. Kasahara (Kyoritsu College of Pharmacy, Tokyo, Japan) for providing HEK293T cells. We also thank R. Izawa and M. Mato for excellent technical support, and K. Kishi (all Jichi Medical University) for advice on statistical analysis. N. Mato (Jichi Medical University) thanks Jichi Medical University for awarding this research the Young Investigator Award.

REFERENCES

1 Bedrossian CW. Iatrogenic and toxic injury. *In*: Dail DH, Hammar SP, eds. Pulmonary Pathology. New York, Springer-Verlag, 1988; pp. 511–517.
2 Ware LB, Matthay MA. The acute respiratory syndrome. *N Engl J Med* 2000; 342: 1334–1349.
3 Tominaga S. A putative protein of a growth specific cDNA from BALB/c-3T3 cells is highly similar to the extracellular portion of mouse interleukin 1 receptor. *FEBS Lett* 1989; 258: 301–304.
4 Tominaga S, Kuroiwa K, Tago K, *et al.* Presence of expression of novel variant form of ST2 gene product in human leukemic cell line UT-7/GM. *Biochem Biophys Res Commun* 1999; 264: 14–18.
5 Schmitz J, Owyang A, Oldham E, *et al.* IL-33, an interleukin-1-like cytokine that signals *via* the IL-1 receptor-related protein ST2 and induces T helper type 2-associated cytokines. *Immunity* 2005; 23: 479–490.
6 Brunner M, Krenn C, Roth G, *et al.* Increased levels of soluble ST2 protein and IgG1 production in patients with sepsis and trauma. *Intensive Care Med* 2004; 30: 1468–1473.
7 Oshikawa K, Yanagisawa K, Tominaga S, *et al.* ST2 protein induced by inflammatory stimuli can modulate acute lung inflammation. *Biochem Biophys Res Commun* 2002; 299: 18–24.
8 Tajima S, Oshikawa K, Tominaga S, *et al.* The increase in serum soluble ST2 protein upon acute exacerbation of idiopathic pulmonary fibrosis. *Chest* 2003; 124: 1206–1214.
9 Sweet MJ, Leung BP, Kang D, *et al.* A novel pathway regulating lipopolysaccharide-induced shock by ST2/T1 *via* inhibition of Toll-like receptor 4 expression. *J Immunol* 2001; 166: 6633–6639.
10 Takezako N, Hayakawa M, Hayakawa H, *et al.* ST2 suppresses IL-6 production *via* the inhibition of IκB degradation induced by the LPS signal in THP-1 cells. *Biochem Biophys Res Commun* 2006; 341: 425–432.
11 Leung BP, Xu D, Culshaw S, *et al.* A novel therapy of murine collagen-induced arthritis with soluble T1/ST2. *J Immunol* 2004; 173: 145–150.
12 Takagi T, Yanagisawa K, Tsukamoto T, *et al.* Identification of the product of the murine ST2 gene. *Biochim Biophys Acta* 1993; 1178: 194–200.
13 Inoue S, Hakamata Y, Kaneko M, *et al.* Gene therapy for organ grafts using rapid injection of naked DNA: application to the rat liver. *Transplantation* 2004; 77: 997–1003.
14 Hakamata Y, Murakami T, Kobayashi E. "Firefly rats" as an organ/cellular source for long-term *in vivo* bioluminescent imaging. *Transplantation* 2006; 81: 1179–1184.
15 Howell DC, Johns RH, Lasky JA, *et al.* Absence of proteinase-activated receptor-1 signaling affords protection from bleomycin-induced lung inflammation and fibrosis. *Am J Pathol* 2005; 166: 1353–1365.
16 Kelley J, Newman RA, Evans JN. Bleomycin-induced pulmonary fibrosis in the rat. Prevention with an inhibitor of collagen synthesis. *J Lab Clin Med* 1980; 96: 954–964.
17 Lindenschmidt RC, Tryka AF, Godfrey GA, *et al.* Intratracheal *versus* intravenous administration of bleomycin in mice: acute effects. *Toxicol Appl Pharmacol* 1986; 85: 69–77.
18 Tajima S, Bando M, Ohno S, *et al.* ST2 gene induced by type 2 helper T cell (Th2) and proinflammatory cytokine stimuli may modulate lung injury and fibrosis. *Exp Lung Res* 2007; 33: 81–97.
19 Zhang G, Budker V, Wolff JA. High levels of foreign gene expression in hepatocytes after tail vein injections of naked plasmid DNA. *Hum Gene Ther* 1999; 10: 1735–1737.
20 Piguet PF, Collart MA, Grau GE, *et al.* Tumor necrosis factor/cachectin plays a key role in bleomycin-induced pneumopathy and fibrosis. *J Exp Med* 1989; 170: 655–663.
21 Jordana M, Richards C, Irving LB, *et al.* Spontaneous *in vitro* release of alveolar-macrophage cytokines after the intratracheal instillation of bleomycin in rats. Characterization and kinetic studies. *Am Rev Respir Dis* 1988; 137: 1135–1140.
22 Kuroiwa K, Arai T, Okazaki H, *et al.* Identification of human ST2 protein in the sera of patients with autoimmune diseases. *Biochem Biophys Res Commun* 2001; 284: 1104–1108.
23 Trajkovic V, Sweet MT, Xu D. T1/ST2 – an IL-1 receptor-like modulator of immune responses. *Cytokine Growth Factor Rev* 2004; 15: 87–95.
24 Amatucci A, Novobrantseva T, Gilbride K, *et al.* Recombinant ST2 boosts hepatic Th2 response *in vivo*. *J Leukoc Biol* 2007; 82: 124–132.

25 Kurowska-Stolarska M, Kewin P, Murphy G, *et al.* IL-33 induces antigen-specific IL-5+ T cells and promotes allergic-induced airway inflammation independent of IL-4. *J Immunol* 2008; 181: 4780–4790.

26 Dunsmore SE, Roes J, Chua FJ, *et al.* Evidence that neutrophil elastase-deficient mice are resistant to bleomycin-induced fibrosis. *Chest* 2001; 120: 35S–36S.

27 Gasse P, Mary C, Guenon I, *et al.* IL-1R1/MyD88 signaling and the inflammasome are essential in pulmonary inflammation and fibrosis in mice. *J Clin Invest* 2007; 117: 3786–3799.

28 Townsend MJ, Fallon PG, Matthews DJ, *et al.* T1/ST2-deficient mice demonstrate the importance of T1/ST2 in developing primary T helper cell type 2 responses. *J Exp Med* 2000; 191: 1069–1076.

Lung (2009) 187:331–339
DOI 10.1007/s00408-009-9162-6

INTERSTITIAL LUNG DISEASE

Effects of IS-741, a Synthetic Anti-Inflammatory Agent, on Bleomycin-Induced Lung Injury in Mice

Yuichi Shimaoka · Shunji Tajima · Fumio Fujimori · Cristiane Yamabayashi · Hiroshi Moriyama · Masaki Terada · Toshinori Takada · Eiichi Suzuki · Masashi Bando · Yukihiko Sugiyama · Ichiei Narita

Received: 3 April 2009 / Accepted: 21 July 2009 / Published online: 13 August 2009

Abstract Bleomycin (BLM)-induced lung injury consists of excessive inflammatory cell infiltration and fibrosis. IS-741 has been reported to be an anti-inflammatory drug through an inhibitory action on cell adhesion. In this study we investigated whether IS-741 could inhibit the progression of pulmonary fibrosis through inflammatory cell infiltration. Lung injury was induced in female C57BL/6 mice by intratracheal instillation of BLM. IS-741 was administered daily intraperitoneally. The hydroxyproline content and fluid content in the lung on Day 28 were significantly lower in the IS-741-treated mice. The histological degree of lung injury or fibrosis was reduced in IS-741-treated mice. Administration of IS-741 caused significant reduction in the absolute number of total cells, monocyte chemoattractant protein (MCP)-1, and cysteinyl leukotriene (cysLTs) levels in bronchoalveolar lavage fluid on Day 7. Furthermore, the hydroxyproline content was significantly lower in IS-741-treated mice even though IS-741 was started on Day 14 after BLM instillation. Treatment with IS-741 had an inhibitory effect on BLM-induced lung injury and fibrosis via the repression of MCP-1 or cysLTs in this murine experimental model.

Y. Shimaoka · S. Tajima (✉) · F. Fujimori · C. Yamabayashi · H. Moriyama · M. Terada · T. Takada · E. Suzuki · I. Narita
Division of Respiratory Medicine, Graduate School of Medical and Dental Sciences, Niigata University, 1-757 Asahimachi-dori, Chuo-ku, Niigata 951-8510, Japan
e-mail: tajimash@med.niigata-u.ac.jp

M. Bando · Y. Sugiyama
Division of Pulmonary Medicine, Department of Medicine, Jichi Medical University, 3311-1 Yakushiji, Shimotsuke, Tochigi 329-0498, Japan

Keywords Bleomycin · IS-741 · Lung injury · Monocyte chemoattractant protein-1 · Pulmonary fibrosis · Cysteinyl leukotrienes

Introduction

It is generally accepted that fibrosis is not a mere end-product of chronic injury, but an active, dynamic process that may be reversible in the early stage of the injury. Moreover, it is supposed that accumulation of leukocytes in the inflamed site and their subsequent interaction with resident fibroblasts might be important in various forms of organic fibrosis [1–5]. Idiopathic pulmonary fibrosis (IPF) is defined as a specific form of chronic fibrosing interstitial pneumonia limited to the lung [6]. The etiology of IPF is not known and it remains a devastating disease with a more than 50% 5-year mortality rate [6]. Unfortunately, the pathogenesis of IPF is also incompletely understood. Although several drugs have been used or tried for treating IPF, there is no established treatment that definitely improves its outcome [6]. Thus, we await new therapies based on a new understanding of the pathogenesis of IPF.

The *N*-(2-ethylsulfonyl-amino-5-trifluoromethyl-3-pyridinyl) carboxamide derivative IS-741 is reported to have an inhibitory effect on cytosolic phospholipase A_2 ($cPLA_2$) and attenuates experimental acute pancreatitis in dogs [7, 8]. IS-741 was also shown to inhibit the expression of macrophage antigen (Mac)-1 (CD11b/CD18) or lymphocyte function-associated antigen (LFA)-1 (CD11a/CD18), a cell adhesion molecule on the surface of circulating neutrophils, and block the adhesion between inflammatory cells and microvascular endothelial cells in vivo and in vitro [9, 10]. In previous studies it was demonstrated that treatment with IS-741 significantly attenuated inflammation in

various inflammatory experimental models such as acute pancreatitis [10–12], ileitis [13], and colitis [9, 14]. The mechanism by which IS-741 prevents the development of acute pancreatitis and colitis might be its inhibitory effect on the adhesion of neutrophils to endothelial cells and subsequent neutrophil infiltration into the pancreatic tissue or intestinal mucosa of the colon. Recently, Kaku et al. [15] have shown that IS-741 attenuates local migration of monocytes and subsequent pancreatic fibrosis via decreased mRNA expressions of monocyte chemoattractant protein (MCP)-1 and LFA-1 in experimental chronic pancreatitis induced by dibutyltin dichloride in rats. Although there are some publications about the effect of IS-741 on the various inflammatory or fibrotic experimental models as above, there are no reports on the effect of IS-741 on the bleomycin (BLM)-induced pulmonary fibrosis model.

Thus, in the present study the established model of BLM-induced lung injury in mice was used to investigate IS-741's inhibition of BLM-induced inflammation and fibrosis.

Materials and Methods

Mice and Reagents

All mice received humane care in accordance with the Guide for the Care and Use of Laboratory Animals, published by the US National Institutes of Health (NIH publication 8523, revised 1985; http://www.nyu.edu/uawc/Forms/Guide-excerpts.pdf). The study protocol was approved by the Ethics Committee for animal experiments of Niigata University, Niigata, Japan. Specific pathogen-free female C57BL/6 mice, 6–8 weeks of age, were obtained from Japan SLC (Niigata, Japan) and housed in the animal facility of Niigata University. BLM was purchased from Nippon Kayaku (Tokyo, Japan). IS-741 was kindly supplied by Ishihara Sangyo Ltd (Osaka, Japan). IS-741 in 1 ml of normal saline was administered intraperitoneally to the mice at a dose of 10 mg/kg/day.

BLM-Induced Pulmonary Fibrosis Model

We used C57BL/6 mice because they are a well-characterized inbred strain that is susceptible to BLM-induced lung injury. To induce pulmonary fibrosis, we treated C57BL/6 mice with intratracheal BLM on Day 0. The C57BL/6 mice were anesthetized by the intraperitoneal administration of 0.01 ml/g 10% pentobarbital sodium solution (Abbott Laboratories, North Chicago, IL, USA), followed by intratracheal instillation of 3 mg BLM/kg body weight in 50 μl of sterile isotonic saline. The control animals received intratracheal saline only.

The mice were randomly divided into six study groups as shown in Fig. 1: (A) the BLM group received normal saline intraperitoneally and intratracheal BLM injection; (B) the BLM + IS-741 group received IS-741 intraperitoneally for 5 weeks and intratracheal BLM injection; (C) the IS-741 group received IS-741 intraperitoneally and intratracheal saline injection; (D) the Control group received normal saline for 5 weeks and saline instillation; (E) the BLM + IS-741 (Anti-inflammatory) group received IS-741 intraperitoneally from Day -7 to Day 14 and intratracheal BLM injection; and (F) the BLM + IS-741 (Anti-fibrotic) group received IS-741 intraperitoneally from Day 14 to Day 28 and intratracheal BLM injection. To examine the time kinetics of the effects of IS-741, mice were treated separately with IS-741 from Days -7 to 14 (early treatment = Anti-inflammatory) or Days 14 to 28 (late treatment = Anti-fibrotic), as previously described [16, 17]. For examination, the mice were killed by drawing blood from the right atrium under anesthesia. Bronchoalveolar lavage (BAL) and histopathology were performed on Day 7. Hydroxyproline assay, histopathological examinations, and measurement of fluid content were performed on surviving mice on Day 28. The experiments of the sampling at Day 7 and the sampling at Day 28 were performed independently, as described in Fig. 1.

Morphological Evaluation

The right lung was removed with the left main bronchus ligation and fixed by filling the lung through a tracheal cannula to 25 cmH_2O with 10% neutral buffered formaldehyde solution. The trachea was then occluded and fixation was allowed to continue for 4–10 days prior to the study. Longitudinal tissue sections of the lung were embedded in paraffin, stained with hematoxylin-eosin (HE), and examined by light microscopy at a magnification of ×100. Each histopathological experiment was performed in at least three or four mice per group.

Measurement of Hydroxyproline or Fluid Content of the Lung

Hydroxyproline content (μg/lung) in the left lung of each subject was assayed according to the commonly used procedure of colorimetric measurement (Mitsubishi Kagaku Bio-Clinical Laboratories, Inc., Tokyo, Japan). Briefly, lungs were harvested on each designated day after BLM administration and homogenized in 1 ml of PBS (pH 7.4) with a tissue tearer. A 1.5-ml volume of each sample (left lung) was then digested in 1 ml of 6 N hydrochloric acid (HCl) for 8 h at 120°C. Five microliters of citrate-acetate buffer (5% citric acid, 7.24% sodium acetate, 3.4% sodium hydroxide, and 1.2% glacial acetic acid, pH 6.0)

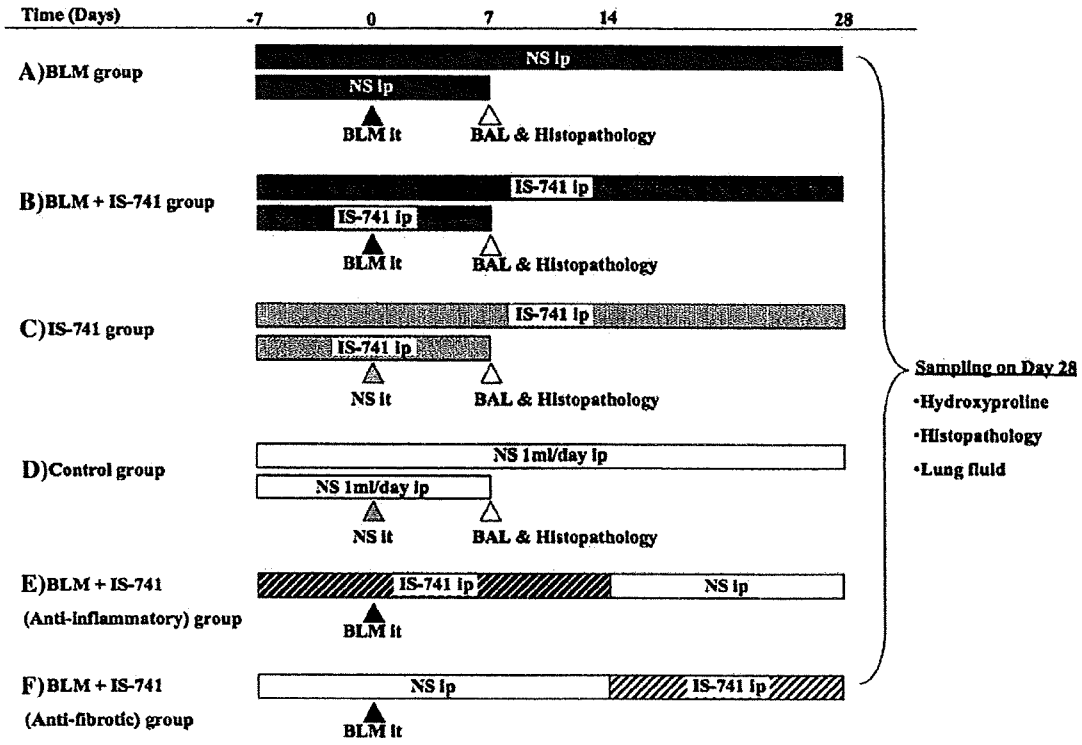

Fig. 1 Experimental designs to determine the activity of IS-741 as an inhibitory agent in the bleomycin (BLM) model. Mice were intratracheally (it) administered BLM or normal saline (NS). IS-741 was administered intraperitoneally (ip). The BLM group received intratracheal BLM injection (A). The BLM + IS-741 group received IS-741 for 5 weeks (B). The IS-741 group (C) and the Control group (D) received intratracheal NS injections. The BLM + IS-741 (Anti-inflammatory) group received IS-741 from Day -7 to Day 14 (E). The BLM + IS-741 (Anti-fibrotic) group received IS-741 from Day 14 to Day 28 (F). The samplings of bronchoalveolar lavage (BAL) fluid at Day 7 and hydroxyproline contents at Day 28 were performed as independent studies

and 100 ml of chloramine-T solution (282 mg of chloramines-T, 2 ml of *n*-propanol, 2 ml of H_2O, and 16 ml of citrate-acetate buffer) were added to each 5-ml sample and the samples were left at room temperature for 20 min. Next, 100 ml of Ehrlich's solution, 9.3 ml of *n*-propanol, and 3.9 ml of 70% perchloric acid were added to each sample and the samples were incubated for 15 min at 65°C. Samples were cooled for 10 min and read at 550 nm on a spectrophotometer. Hydroxyproline concentrations from 0 to 400 mg/ml were utilized to construct a standard curve.

The wet lung weight of the left lobe was measured after careful excision of extraneous tissues. The lung was exposed for 48 h at 180°C and the dry weight measured. Water content was calculated by subtraction of the dry weight from the wet weight.

Sampling of BAL Fluid

BAL was performed through a tracheal cannula to the right lung with 0.5 ml of saline four times, with the left main bronchus ligation. In each mouse examined, approximately 1.8 ml (90%) of BAL fluid (BALF) was recovered. A 100-μl aliquot was used for the total cell count, and the remainder was immediately centrifuged at 1000 *g* for 10 min. The total cell count was made using a hemocytometer, and cell differentiation was determined for more than 500 cells on cytocentrifuge slides with Wright-Giemsa staining. The supernatants of BALF were stored at −80°C until used.

Assays for $cPLA_2$ Products and MCP-1 in BALF

Thromboxane (Tx) A_2 measured as TxB_2, leukotriene (LT) B_4, and cysteinyl leukotrienes (cysLTs) in BALF were determined by using enzyme immunoassay (EIA) kits (Amersham Pharmacia Biotech, Piscataway, NJ, USA). MCP-1 in BALF was measured by the Mouse MCP-1 Immunoassay kit (Biosource International, Camarillo, CA, USA).

Flow Cytometry of LFA-1 (CD11a/CD18) in BAL Cells

Suspended BAL cells in PBS from the three groups (the BLM group, the BLM + IS-741 group, and the Control

group) were stained with fluorescein isothiocyanate-, phycoerythrin-, or pericinin chlorophyll protein-conjugated monoclonal anti-CD11a, CD18, and CD45 antibodies (Becton-Dickinson, San Jose, CA, USA) in phosphate buffer saline for 20 min at 4°C. Stained cells were analyzed on flow cytometry (FACScan; Becton-Dickinson) using a Cell Quest program. Leukocytes were determined using flow cytometric analysis of light scatter chamber characteristics relating to size and granulation, and fluorescence gating with anti-CD45 antibody. Three-color flow cytometry was then performed to calculate the percentages of CD11a and CD18 positive cells in a subset of $CD45^+$ leukocytes.

Statistical Analysis

Survival curves were estimated by the Kaplan–Meier method. Comparisons of all curves were done using the two-tailed log-rank test. Data were expressed as mean ± SEM. For multiple comparisons, we performed a one-way analysis of variance, and then Fisher's protected least-significant differences method was used as a post-hoc test. Values of $P < 0.05$ were considered to indicate statistical significance.

Results

Effects of IS-741 on Mortality in BLM-Treated Mice

Contrary to our expectation, there was no significant difference in the survival rate on Day 28 between the BLM group and the BLM + IS-741 group ($P > 0.05$; 80% vs. 87%, respectively), using a two-tailed log-rank test (Fig. 2). The Control group and the IS-741 group recorded no deaths (Fig. 2).

Analysis of Inflammatory Cell Infiltration to the Lung by Instillation of BLM

Inflammatory cell infiltration into the lung was evaluated by histologic examination and BALF cell analysis on Day 7. Edematous thickening of alveolar septa and the infiltration of neutrophils and macrophages and a few lymphocytes were observed by BLM instillation (Fig. 3a). The alveolitis was less severe in the BLM + IS-741 group than in the BLM group (Fig. 3a, b).

Preadministration of IS-741 significantly reduced the number of total cells in the BALF ($P = 0.018$) (Fig. 3e). In the BALF cell differentiation, macrophages, neutrophils, and lymphocytes tended to be reduced by IS-741 but not significantly (Fig. 3e).

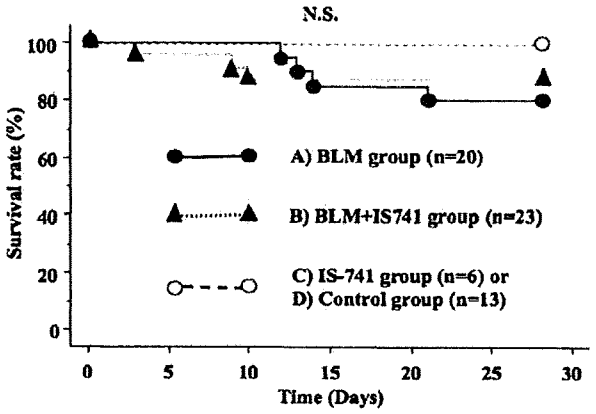

Fig. 2 Effects of IS-741 on mortality in the bleomycin (BLM) model. The survival rates of four study groups of mice are shown over a 28-day observation period. There was no significant difference among the BLM group (●), the BLM + IS-741 group (▲), and the IS-741 group or the control group (○). The described number of each group was a pool of three independent experiments

Administration of IS-741 Ameliorated BLM-Induced Pulmonary Fibrosis or Lung Edema in Mice

The fibrotic change in the lung was evaluated by histological examination and measurement of hydroxyproline contents. As shown in Fig. 4a–f, all three IS-741 administration groups demonstrated significant reduction of fibrosis in the subpleural areas or the around bronchiole of the lung. IS-741 has been reported to be the anti-inflammatory agent, as described above. However, in addition to histologic examination, the hydroxyproline assay demonstrated that IS-741 reduced the total hydroxyproline contents in all three treated groups compared with the BLM-alone group (Fig. 4g).

To evaluate lung edema formation, we measured wet-dry lung weight. Compared with the BLM group, the BLM + IS-741 group significantly reduced the fluid content (Fig. 5).

Effects of IS-741 on the $cPLA_2$ Products and MCP-1 Levels in BALF of the BLM Model

To assess the biosynthesis of $cPLA_2$ products we performed BALF assays of TxB_2, LTB_4, and cysLTs (LTC_4/D_4/E_4). As shown in Fig. 6a, cysLTs level in BLM-treated mice was significantly greater than that in the two groups that did not receive BLM. However, pretreatment with IS-741 significantly decreased the elevated levels of cysLTs in BALF compared with those in the animals treated with BLM alone ($P = 0.006$). For other eicosanoids, BALF levels of TxB_2 or LTB_4 in the BLM + IS-741 group did not differ from those in the BLM group (data not shown).

The MCP-1 level in BALF was measured as an index of the amount of regulating factor of monocyte chemoattractant and infiltration to the lung. As shown in Fig. 6b, the

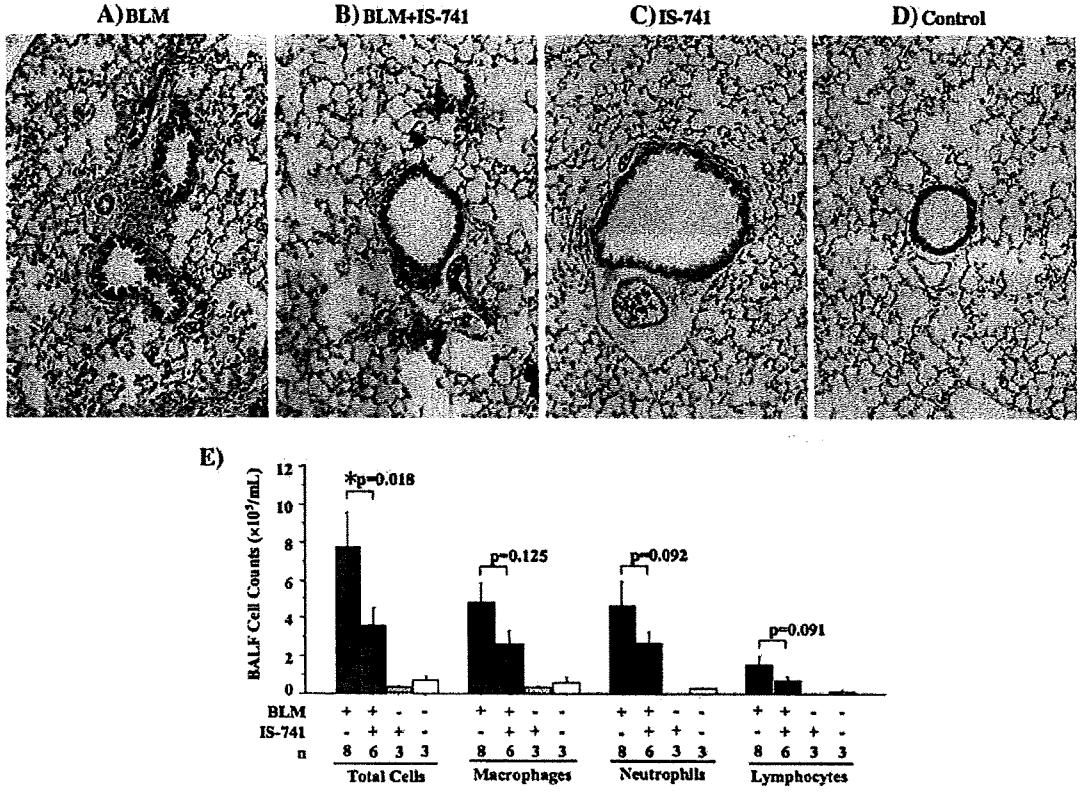

Fig. 3 Effects of IS-741 on acute inflammatory phase in the bleomycin (BLM) model. Lung tissue was obtained on Day 7 and stained with hematoxylin and eosin (original magnification ×100). Alveolar thickening and infiltration of inflammatory cells in the alveolar space are seen in the BLM group (**a**); however, these features are less severe in the BLM + IS-741group (**b**). No histological effect on the lung tissue is observed in the IS-741 group (**c**) compared with the Control group (**d**). On bronchoalveolar lavage fluid findings at Day 7, the number of total cells in the BLM + IS-741 group is significantly decreased compared with that in the BLM group (**e**). No differences have been seen in the IS-741 group compared with the Control group (**e**). Data are presented as the mean ± SEM. $*P < 0.05$ in comparison to the BLM group. Data are representative of three separate experiments

preadministration of IS-741 caused a significant reduction of the elevated levels of MCP-1 in BALF induced by BLM challenge ($P = 0.037$).

Flow Cytometry of LFA-1 (CD11a/CD18) in BAL Cells

Inflammatory cells from BAL were analyzed by flow cytometry to evaluate the expression of surface antigens CD11a and CD18. Although the frequency of $CD11a^+$ or $CD18^+$ cells from BAL of the BLM group was greater than that of the Control group, administration of IS-741 did not affect the percentage of $CD11a^+$ or $CD18^+$ cells from BAL (data not shown).

Discussion

In the present study, a murine BLM-induced pulmonary fibrosis mouse model was used to examine the ability of IS-741 to inhibit pulmonary fibrosis by decreasing lung inflammation and attenuating $cPLA_2$ products or MCP-1 levels. We have shown that IS-741 could mitigate the progression of lung injury and fibrosis. It also attenuated the cellular infiltration and the concentrations of cysLTs and MCP-1 in BALF. These findings suggested that IS-741 could inhibit lung injury and fibrosis via the repression of cysLTs or MCP-1 production in the current model.

A major difference between human IPF and the mouse model is the inflammatory component of early BLM-induced lung injury, which is often absent in human IPF [18]. Chaudhary et al. [19] determined the time course of the development of inflammation and fibrosis in BLM-induced lung fibrosis in rat. They demonstrated that in an animal model that comprised a single intratracheal injection of BLM, the "switch" between inflammation and fibrosis occurred on or just after Day 9 [19]. At first we hypothesized that IS-741 has an only "anti-inflammatory" effect. Despite our expectation, not only the "Anti-inflammatory" group but also the "Anti-fibrotic" group

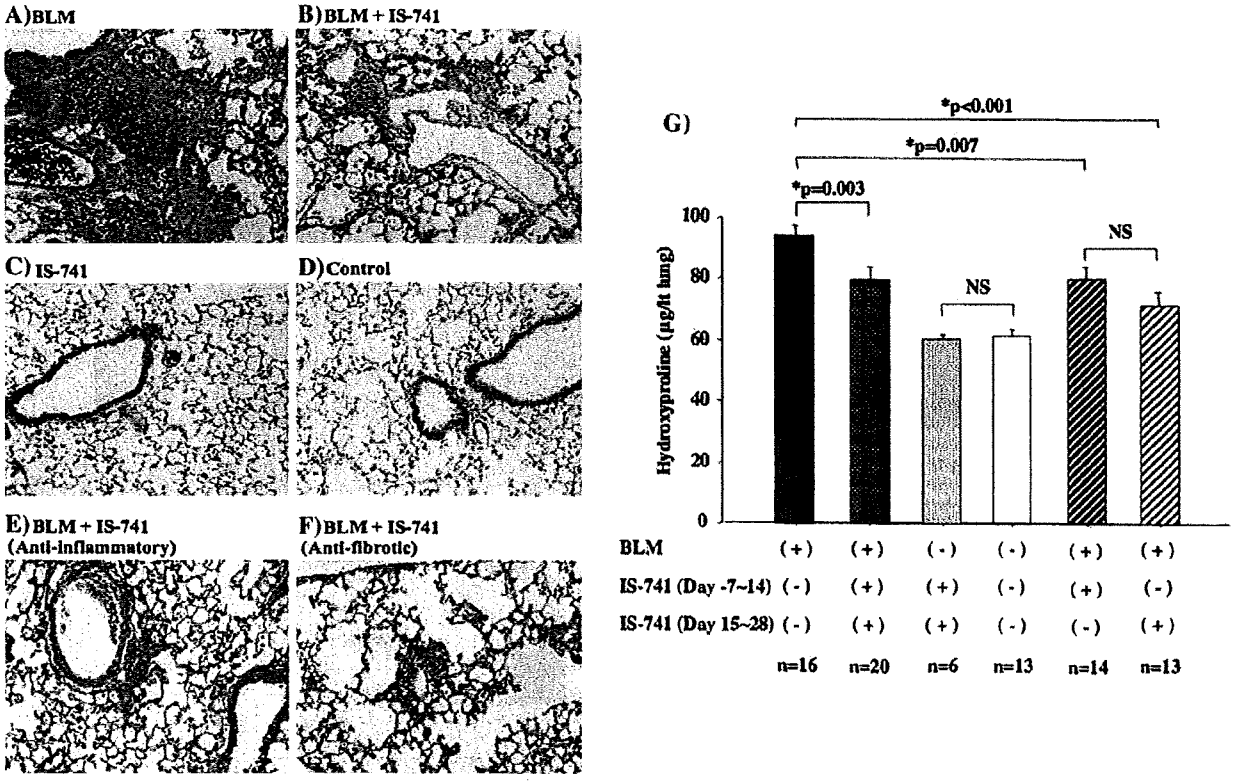

Fig. 4 Effects of IS-741 on chronic fibrotic phase in the bleomycin (BLM) model. Lung tissue was obtained on Day 28 after instillation of BLM or saline and stained with hematoxylin and eosin (original magnification ×100). A lung tissue sample from the BLM group shows alveolitis and patchy fibrosis with destruction of the alveolar structure, mainly in the bronchiole region (**a**). However, these features are less severe in the three IS-741 treatment groups: the BLM + IS-741 group (**b**), the BLM + IS-741 (Anti-inflammatory) group (**e**), and the BLM + IS-741 (Anti-fibrotic) group (**f**). A lung tissue sample from the IS-741 group (**c**) and the Control group (**d**) appear normal. Data are representative of three separate experiments. The BLM + IS-741 group significantly attenuates the BLM-induced increase in hydroxyproline content on Day 28 (**g**). In addition, the BLM + IS-741 (Anti-inflammatory) group and the BLM + IS-741 (Anti-fibrotic) group also significantly decrease hydroxyproline contents (**g**). Data are presented as the mean ± SEM (n = 6–20 in each group). *$P < 0.05$ in comparison to the BLM group. The described number of each group was a pool of three independent experiments. Details of each group protocol are described in Fig. 1

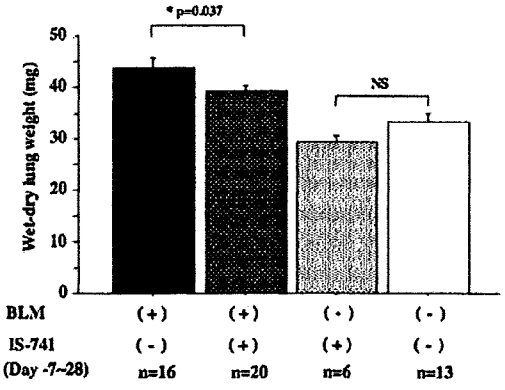

Fig. 5 Effects of IS-741 on fluid contents of the bleomycin (BLM) model. Treatment with IS-741 from Day -7 to Day 28 significantly reduced edema formation induced by BLM. Data are presented as mean ± SEM. The described number of each group was a pool of three independent experiments

could mitigate the progression of pulmonary fibrosis. There are two previous reports on the therapeutic (not preventive) effect of IS-741 on chronic pancreatic fibrosis models [15, 20]. In those studies, to exclude the effect of IS-741 on acute pancreatitis and to evaluate the efficacy on the chronic phase the authors started administration of IS-741 at Day 7 or later after the challenge of dibutyltin dichloride or dibutyltin dichloride, respectively [15, 20]. They reported that pancreatic fibrosis was inhibited by IS-741 administration therapeutically [15, 20]. In vitro study has shown that IS-741 had no direct effect on the proliferation, collagen synthesis, or α smooth muscle actin expression of rat pancreatic stellate cells without MCP-1 production [15]. Further analysis will be needed to determine which cells affect MCP-1 production by IS-741 in the fibrotic lung.

It has been reported that the MCP-1 functional pathway may play an important role in the development of pulmonary fibrosis [21–25]. Although our results indicated

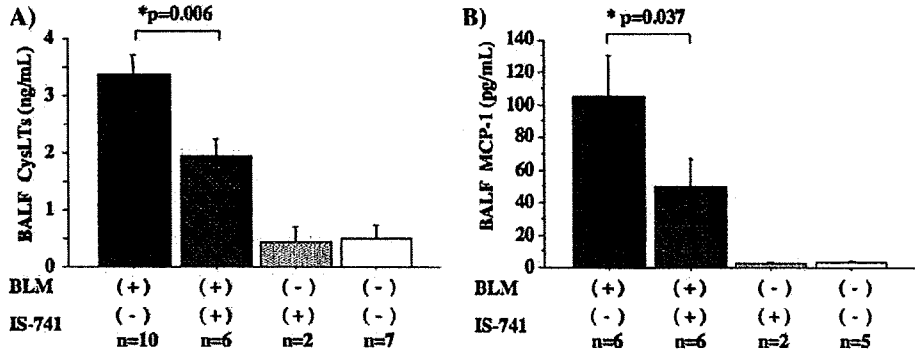

Fig. 6 Effects of IS-741 on the cysteinyl leukotrienes (cysLTs) and monocyte chemoattractant protein (MCP)-1 levels in bronchoalveolar lavage fluid (BALF) in the bleomycin (BLM) model. BALF levels of both cysLTs (**a**) and MCP-1 (**b**) are significantly attenuated in the BLM + IS-741 group in comparison to the BLM group on Day 7. Data are presented as the mean ± SEM. * $P < 0.05$ compared with the BLM group. Data are representative of three separate experiments

that IS-741 might regulate MCP-1 production in the lung of the BLM-induced pulmonary fibrosis model, the exact mechanism of IS-741 responsible for this inhibitory action at the chronic fibrosis phase has not yet been elucidated. Inoshima et al. [26] have shown that overexpression of a mutant MCP-1 gene 10–14 days after intratracheal BLM instillation resulted in decreased DNA damage, apoptosis, and pulmonary fibrosis at 14 days. However, overexpression of the mutant MCP-1 0–4 days after BLM instillation did not decrease the pathological grade, DNA damage, or apoptosis at 7 and 14 days [26]. These findings suggest that MCP-1 might play an important role in the development of fibrogenesis but not in the development of early lung inflammation. Further examination is needed to clarify the antifibrotic function of IS-741 in lung fibrosis.

BLM-induced lung fibrosis was significantly reduced in the 5-lipoxygenase knockout mouse or the $cPLA_2$ knockout mouse by inhibiting cysLTs [27, 28]. These findings suggest that $cPLA_2$ products may have a pivotal role in the development of pulmonary fibrosis. Originally, IS-741 was prepared and evaluated as a $cPLA_2$ inhibitor; however, a high concentration was needed to inhibit $cPLA_2$ activity [7, 8]. The present study demonstrated that IS-741 reduced the elevated levels of cysLTs in BALF. The reduction of cysLTs might mainly be a secondary effect because of the attenuation of the infiltration of inflammatory cells into the lung. In addition, $cPLA_2$-inhibiting activity of IS-741 may also attenuate the production of cysLTs.

Many adhesion molecules are crucial for securing leukocyte-endothelial cell interaction such as the selectin family; the immunoglobulin superfamily, including intercellular adhesion molecule 1 and vascular cell adhesion molecule 1; and the integrin family, including LFA-1, Mac-1, and very late antigen 4 [29]. IS-741 has an inhibitory action against the cell adhesion between leukocytes and microvascular endothelial cells [10, 12, 30]. IS-741 has been reported to inhibit cell adhesion significantly between human umbilical vein endothelial cells and human promyeloleukemia cells during lipopolysaccharide stimulation in vitro [31]. It has been suggested that the exact mechanism of IS-741 responsible for this inhibitory action is that IS-741 inhibits the cluster formation of LFA-1 with the activation of LFA-1 [32]. Our flow cytometry analysis showed that administration of IS-741 did not affect the percentage of $CD11a^+$ or $CD18^+$ cells from BAL in our model. This finding may the support the above hypothesis that IS-741 did not affect the amounts of LFA-1 expression but inhibited the cluster formation of activating LFA-1. Although anti-inflammatory effects of IS-741 on acute inflammation with the infiltration of leukocytes were reported [9, 10, 12–14], effects of IS-741 on chronic inflammation and fibrosis remain unclear.

Yotsuya et al. [33] have shown that the number of infiltrating leukocytes on acute pancreatitis in rats was significantly decreased after treatment with10 mg/kg/day of IS-741 but not after 0.1 or 1 mg/kg/day of IS-741. Therefore, we used IS-741 at a dose of 10 mg/kg/day. Although most studies used 10 mg/kg/day of IS-741 [9, 10, 12, 14], the other studies used IS-741 in large quantities such as 20 mg/kg/day in dogs [8] and 50 mg/kg/day [13, 15], 72 mg/kg/day [11], and 100 mg/kg/day [32] in rats. As shown in Fig. 1, four of 20 mice (20%) in the BLM group died, and three of 23 mice (13%) in the BLM + IS741 group died. One could conclude that the beneficial effects of IS-741 are not significant. We did not explain the exact reason why administration of IS-741 did not affect mortality, but our dose of IS-741 might be slightly small to show the statistically significant attenuation of mortality.

In summary, the results of the present study suggested that IS-741 could inhibit BLM-induced lung injury and fibrosis by the repression of MCP-1 and cysLTs production. These findings suggested that the administration of IS-

741 might therefore modulate the process of pulmonary fibrosis via regulating anti-inflammatory mediator production. However, the precise mechanism by which IS-741 modulates lung injury and/or fibrosis remains obscure. Further studies are thus required to elucidate this issue.

Acknowledgments This study was supported by the Health and Labour Sciences Research Grants on Diffuse Lung Diseases from the Japanese Ministry of Health, Labour and Welfare, Grant for Promotion of Niigata University Research Projects (90), and Research Grant from Shimane University Medical School Alumni Association.

References

1. Kuwahara F, Kai H, Tokuda K, Niiyama H, Tahara N, Kusaba K, Takemiya K, Jalalidin A, Koga M, Nagata T, Shibata R, Imaizumi T (2003) Roles of intercellular adhesion molecule-1 in hypertensive cardiac remodeling. Hypertension 41:819–823
2. Chow FY, Nikolic-Paterson DJ, Ozols E, Atkins RC, Tesch GH (2005) Intercellular adhesion molecule-1 deficiency is protective against nephropathy in type 2 diabetic db/db mice. J Am Soc Nephrol 16:1711–1722
3. Blaber R, Stylianou E, Clayton A, Steadman R (2003) Selective regulation of ICAM-1 and RANTES gene expression after ICAM-1 ligation on human renal fibroblasts. J Am Soc Nephrol 14:116–127
4. Imamura M, Ogawa T, Sasaguri Y, Chayama K, Ueno H (2005) Suppression of macrophage infiltration inhibits activation of hepatic stellate cells and liver fibrogenesis in rats. Gastroenterology 128:138–146
5. Huo Y, Ley K (2001) Adhesion molecules and atherogenesis. Acta Physiol Scand 173:35–43
6. American Thoracic Society (2000) Idiopathic pulmonary fibrosis: diagnosis and treatment. International consensus statement. American Thoracic Society (ATS), and the European Respiratory Society (ERS). Am J Respir Crit Care Med 161:646–664
7. Kimura H, Yotsuya S, Yuki S, Sugi H, Shigehara I, Haga T (1995) Synthesis and antipancreatitis activities of novel N-(2-sulfonylamino-5-trifluoromethyl-3-pyridyl) carboxamide derivatives as phospholipase A2 inhibitors. Chem Pharm Bull (Tokyo) 43:1696–1700
8. Isaji S, Hayashi J, Higashiguchi T, Yokoi H, Ogura Y, Noguchi T, Kawarada Y (1999) Effect of IS-741 (a new synthetic antiinflammatory agent) on acute necrotizing pancreatitis in dogs. Significance of its inhibitory effect on cytosolic phospholipase A2. Digestion 60(Suppl 1):47–51
9. Makino J, Andoh A, Hata K, Yotsuya S, Shikama H, Araki Y, Fujiyama Y, Bamba T (2002) Suppressive effects of a new anti-inflammatory agent, IS-741, on dextran sulfate sodium-induced experimental colitis in rats. Int J Mol Med 9:391–396
10. Yamauchi J, Sunamura M, Shibuya K, Takeda K, Kobari M, Matsuno S (1999) A novel diamino-pyridine derivative prevents excessive leukocyte infiltration in aggravation of acute necrotizing pancreatitis. Digestion 60(Suppl 1):40–46
11. Yamaguchi Y, Okabe K, Liang J, Matsumura F, Akizuki E, Matsuda T, Ohshiro H, Nakano S, Ishihara K, Ogawa M (1999) The novel carboxamide derivative IS-741 reduces neutrophil chemoattractant production by bronchoalveolar macrophages in rats with cerulein-induced pancreatitis complicated by sepsis. Digestion 60(Suppl 1):52–56
12. Imamura T, Niikawa J, Kitamura K, Takahashi A, Ikegami A, Yoshida H, Tanaka S, Mitamura K (2003) Effect of IS-741 on ethionine-induced acute pancreatitis in rats: relation to pancreatic acinar cell regeneration. J Gastroenterol 38:260–267
13. Fukunaga T, Tsujikawa T, Sasaki M, Fujiyama Y, Bamba T, Fujimiya M (2003) A novel diamino-pyridine derivative (IS-741) attenuates rat ileitis induced by trinitrobenzene sulfonic acid. J Gastroenterol 38:451–459
14. Makino J, Andoh A, Hata K, Yotsuya S, Shikama H, Imamura M, Fujiyama Y, Bamba T (2002) Inhibitory effects of the new anti-inflammatory agent, IS-741, on spontaneous colitis in HLA-B27/beta2-microglobulin transgenic rats. J Gastroenterol Hepatol 17:854–860
15. Kaku T, Oono T, Zhao H, Gibo J, Kawabe K, Ito T, Takayanagi R (2007) IS-741 attenuates local migration of monocytes and subsequent pancreatic fibrosis in experimental chronic pancreatitis induced by dibutyltin dichloride in rats. Pancreas 34:299–309
16. Aono Y, Nishioka Y, Inayama M, Ugai M, Kishi J, Uehara H, Izumi K, Sone S (2005) Imatinib as a novel antifibrotic agent in bleomycin-induced pulmonary fibrosis in mice. Am J Respir Crit Care Med 171:1279–1285
17. Azuma M, Nishioka Y, Aono Y, Inayama M, Makino H, Kishi J, Shono M, Kinoshita K, Uehara H, Ogushi F, Izumi K, Sone S (2007) Role of alpha1-acid glycoprotein in therapeutic antifibrotic effects of imatinib with macrolides in mice. Am J Respir Crit Care Med 176:1243–1250
18. Selman M, King TE, Pardo A (2001) Idiopathic pulmonary fibrosis: prevailing and evolving hypotheses about its pathogenesis and implications for therapy. Ann Intern Med 134:136–151
19. Chaudhary NI, Schnapp A, Park JE (2006) Pharmacologic differentiation of inflammation and fibrosis in the rat bleomycin model. Am J Respir Crit Care Med 173:769–776
20. Xie MJ, Motoo Y, Su SB, Iovanna JL, Sawabu N (2002) Effect of carboxamide derivative IS-741 on rat spontaneous chronic pancreatitis. Dig Dis Sci 47:139–147
21. Antoniades HN, Neville-Golden J, Galanopoulos T, Kradin RL, Valente AJ, Graves DT (1992) Expression of monocyte chemoattractant protein-1 mRNA in human idiopathic pulmonary fibrosis. Proc Natl Acad Sci USA 89:5371–5375
22. Iyonaga K, Takeya M, Saita N, Sakamoto O, Yoshimura T, Ando M, Takahashi K (1994) Monocyte chemoattractant protein-1 in idiopathic pulmonary fibrosis and other interstitial lung diseases. Hum Pathol 25:455–463
23. Car BD, Meloni F, Luisetti M, Semenzato G, Gialdroni-Grassi G, Walz A (1994) Elevated IL-8 and MCP-1 in the bronchoalveolar lavage fluid of patients with idiopathic pulmonary fibrosis and pulmonary sarcoidosis. Am J Respir Crit Care Med 149:655–659
24. Suga M, Iyonaga K, Ichiyasu H, Saita N, Yamasaki H, Ando M (1999) Clinical significance of MCP-1 levels in BALF and serum in patients with interstitial lung diseases. Eur Respir J 14:376–382
25. Zhang K, Gharaee-Kermani M, Jones ML, Warren JS, Phan SH (1994) Lung monocyte chemoattractant protein-1 gene expression in bleomycin induced pulmonary fibrosis. J Immunol 153:4733–4741
26. Inoshima I, Kuwano K, Hamada N, Hagimoto N, Yoshimi M, Maeyama T, Takeshita A, Kitamoto S, Egashira K, Hara N (2004) Anti-monocyte chemoattractant protein-1 gene therapy attenuates pulmonary fibrosis in mice. Am J Physiol Lung Cell Mol Physiol 286:L1038–L1044
27. Peters-Golden M, Bailie M, Marshall T, Wilke C, Phan SH, Toews GB, Moore BB (2002) Protection from pulmonary fibrosis in leukotriene-deficient mice. Am J Respir Crit Care Med 165:229–235
28. Nagase T, Uozumi N, Ishii S, Kita Y, Yamamoto H, Ohga E, Ouchi Y, Shimizu T (2002) A pivotal role of cytosolic phospholipase A(2) in bleomycin-induced pulmonary fibrosis. Nat Med 8:480–484
29. Salmi M, Jalkanen S (2005) Cell-surface enzymes in control of leukocyte trafficking. Nat Rev Immunol 5:760–771

30. Hamaguchi Y, Nishizawa Y, Yasui M, Hasegawa M, Kaburagi Y, Komura K, Nagaoka T, Saito E, Shimada Y, Takehara K, Kadono T, Steeber DA, Tedder TF, Sato S (2002) Intercellular adhesion molecule-1 and L-selectin regulate bleomycin-induced lung fibrosis. Am J Pathol 161:1607–1618
31. Shikama H, Yotsuya S, Satake S, Sugi H, Kato M (1999) Effect of IS-741 on cell adhesion between human umbilical vein endothelial cells and HL-60 cells. Biol Pharm Bull 22:127–131
32. Yotsuya S, Shikama H, Imamura M (2001) Efficacy of the inflammatory cell infiltration inhibitor IS-741 on colitis induced by dextran sulfate sodium in the rat. Jpn J Pharmacol 87:151–157
33. Yotsuya S, Shikama H, Nakano I, Sakai K, Kato M, Sugi H, Takada H, Koga Y (1999) A novel synthetic anti-acute pancreatitis agent, IS-741. Digestion 60(Suppl 1):34–39

The American Journal of Pathology, Vol. 176, No. 3, March 2010

DOI: 10.2353/ajpath.2010.091057

Correspondence

EML4-ALK Fusion in Lung

To the Editor-in-Chief:

The recent article by Martelli and colleagues[1] reports (i) the detection of *EML4-ALK* fusion cDNA[2] not only in non-small cell lung cancer (NSCLC) specimens but in non-tumor lung tissues, (ii) a very low proportion of FISH-positive cells for *ALK* rearrangements among *EML4-ALK*–positive specimens, and (iii) the failure to detect EML4-ALK protein by immunohistochemistry (IHC) and Western blotting. Based on these lines of observation, the authors questioned the clinical relevance of *EML4-ALK* in the carcinogenesis of NSCLC.

Although detection of fusion kinases in normal tissues is a potentially interesting observation, caution is warranted in the interpretation of their results.[1,3] They replicated thrice the reverse transcription-polymerase chain reaction (RT-PCR) for *EML4-ALK* and noted that "In half of the (positive) cases, one replicate experiment did not confirm the fusion transcript was present." They then suggested that the fusion gene was "expressed at very low level." It is, however, also quite possible that such unstable PCR results may simply represent contaminated experiments. If this is the case, a discussion on FISH and protein analyses would become irrelevant. In their report, the presence of the *EML4-ALK* fusion gene was only evidenced by unstable RT-PCR results and a small proportion of FISH-positive cells among specimens.

In this regard, it was surprising that the authors had not tried genomic PCR to exclude the possibility of PCR contamination.[1,3] In most of their fusion-positive cases, they found the *EML4-ALK* variant 1 cDNA, in which exon 13 of *EML4* cDNA is connected to exon 20 of *ALK* cDNA. Because the length of intron 14 of *EML4* gene and intron 19 of *ALK* gene is 5724 bp and 1932 bp, respectively, the maximum size of the genomic PCR to detect the gene fusion should be ≈7.7 kbp, which is within the scope of current long-range PCR systems. Indeed, we have been able to detect genomic PCR products among >50% of the fusion cDNA-positive cases. Interestingly, the break/fusion points in the genome vary substantially among NSCLC specimens,[2,4,5] and we have not obtained, to date, any pairs of NSCLC specimens carrying identical break/fusion points in their genome (even among those positive for the same *EML4-ALK* variants).

We speculate, therefore, that (i) if none of the fusion cDNA-positive cases reported by Martelli et al[1,3] produce specific genomic PCR products, then the fusion cDNA products likely arose from cDNA-contamination, (ii) if the fusion cDNA–positive cases yield identical genomic PCR products, then the fusion cDNAs likely arose from specimen-contamination, and (iii) if the fusion cDNA-positive cases display distinct genomic fusion points, then each specimen was truly positive for the *EML4-ALK* fusion gene. Without such careful examination, we have to conclude that their claims in the article have not as yet been clearly demonstrated.

As described previously,[6] immunohistochemical detection of the EML4-ALK protein is highly difficult, probably owing to the weak activity of the *EML4* promoter that drives the expression of *EML4-ALK* messages. We have thus examined the suitability of commercially available antibodies to ALK for IHC and successfully developed the intercalated antibody–enhanced polymer (iAEP) method, which enables reliable detection of EML4-ALK among formalin-fixed and paraffin-embedded specimens.[6] The same specimen positive for *EML4-ALK* RT-PCR can be, for instance, readily stained to be positive with iAEP, but negative with conventional IHC methods (see Supplemental Figure S1 in ref. 6). We thus agree with Martelli et al that screening of NSCLC specimens with conventional IHC methods will not detect EML4-ALK protein, but strongly argue that such failure does not simply indicate the absence of EML4-ALK. For such screening, we recommend iAEP or other sensitive techniques.[7]

It should be further noted that, in both our[6] and other researchers' IHC analyses,[7] almost all tumor cells in a given *EML4-ALK*–positive specimen were positively immunostained with anti-ALK antibodies, suggesting a homogenous presence of *EML4-ALK* within a tumor. Such observation is, however, in contrast to the FISH data by Martelli et al, which show that the *ALK* rearrangement was only positive in ≈2% of tumor cells in a given *EML4-ALK*–positive specimen. On the contrary, FISH analyses of our *EML4-ALK*–positive samples clearly demonstrate that most of the tumor cells harbor rearranged *ALK* alleles, implying that the generation of the *EML4-ALK* fusion gene is an early event in NSCLC carcinogenesis. The homogenous presence of EML4-ALK in our fusion-positive tumors, as demonstrated by both FISH and IHC, further raises a concern about the "EML4-ALK–positive tumors" as defined by Martelli et al.

Specific inhibitors to ALK enzymatic activity are already in clinical trial, as reported at the 2009 annual meeting of America Society of Clinical Oncology and the European Cancer Organization and Congress of the European Soci-

ety for Medical Oncology.[8] Such reports reveal only modest and transient side effects (nausea, vomiting, and diarrhea) with their ALK inhibitor, but without severe damage in hematopoiesis or renal function. On the other hand, the marked therapeutic efficacy of their compound against EML4-ALK–positive NSCLC makes it one of the rare, highly successful molecular targeted therapies against human cancer, in line with imatinib mesylate and gefitinib/erlotinib. These data further reinforce the essential role of EML4-ALK in the carcinogenesis of NSCLC, and question the validity of the conclusions led by Martelli et al.[1,3]

Hiroyuki Mano
Kengo Takeuchi

Jichi Medical University, Tochigi, Japan
The University of Tokyo, Tokyo, Japan
The Cancer Institute, Tokyo, Japan

References

1. Martelli MP, Sozzi G, Hernandez L, Pettirossi V, Navarro A, Conte D, Gasparini P, Perrone F, Modena P, Pastorino U, Carbone A, Fabbri A, Sidoni A, Nakamura S, Gambacorta M, Fernandez PL, Ramirez J, Chan JK, Grigioni WF, Campo E, Pileri SA, Falini B: EML4-ALK rearrangement in non-small cell lung cancer and non-tumor lung tissues. Am J Pathol 2009, 174:661–670
2. Soda M, Choi YL, Enomoto M, Takada S, Yamashita Y, Ishikawa S, Fujiwara S, Watanabe H, Kurashina K, Hatanaka H, Bando M, Ohno S, Ishikawa Y, Aburatani H, Niki T, Sohara Y, Sugiyama Y, Mano H: Identification of the transforming *EML4-ALK* fusion gene in non-small-cell lung cancer. Nature 2007, 448:561–566
3. Sozzi G, Martelli MP, Conte D, Modena P, Pettirossi V, Pileri SA, Falini B: The EML4-ALK transcript but not the fusion protein can be expressed in reactive and neoplastic lymphoid tissues. Haematologica 2009, 94:1307–1311
4. Choi YL, Takeuchi K, Soda M, Inamura K, Togashi Y, Hatano S, Enomoto M, Hamada T, Haruta H, Watanabe H, Kurashina K, Hatanaka H, Ueno T, Takada S, Yamashita Y, Sugiyama Y, Ishikawa Y, Mano H: Identification of novel isoforms of the *EML4-ALK* transforming gene in non-small cell lung cancer. Cancer Res 2008, 68:4971–4976
5. Takeuchi K, Choi YL, Soda M, Inamura K, Togashi Y, Hatano S, Enomoto M, Takada S, Yamashita Y, Satoh Y, Okumura S, Nakagawa K, Ishikawa Y, Mano H: Multiplex reverse transcription-PCR screening for *EML4-ALK* fusion transcripts. Clin Cancer Res 2008, 14:6618–6624
6. Takeuchi K, Choi YL, Togashi Y, Soda M, Hatano S, Inamura K, Takada S, Ueno T, Yamashita Y, Satoh Y, Okumura S, Nakagawa K, Ishikawa Y, Mano H: KIF5B-ALK, a novel fusion oncokinase identified by an immunohistochemistry-based diagnostic system for ALK-positive lung cancer. Clin Cancer Res 2009, 15:3143–3149
7. Rodig SJ, Mino-Kenudson M, Dacic S, Yeap BY, Shaw A, Barletta JA, Stubbs H, Law K, Lindeman N, Mark E, Janne PA, Lynch T, Johnson BE, Iafrate AJ, Chirieac LR: Unique clinicopathologic features characterize ALK-rearranged lung adenocarcinoma in the western population. Clin Cancer Res 2009, 15:5216–5223
8. Kwak EL, Camidge DR, Clark J, Shapiro GI, Maki RG, Ratain MJ, Solomon B, Bang Y, Ou S, Salgia R: Clinical activity observed in a phase I dose escalation trial of an oral c-met and ALK inhibitor, PF-02341066. J Clin Oncol 2009, 27:15s, (suppl, abstr 3509)

Authors' reply:

In their letter, Mano and Takeuchi claim that our unstable PCR results in normal and cancerous lung tissues could be attribtuable to contamination. However, as clearly illustrated in our article,[1] serial dilution experiments in the H2228 cell line demonstrate the specificity and sensitivity of our RT-PCR assay. Furthermore, the identification in our EML4-ALK fusion positive tissues of alternative isoforms of variant 3, rather than the described two isoforms coexpressed in the H2228 cell line, is indicative of exclusive events in tumors, making contamination unlikely. Lastly, our experiments were confirmed independently in two laboratories (Milan and Barcelona) and always contained appropriate negative PCR controls.

We disagree with Mano et al's claim that the results of genomic PCR could be used to prove a possible RT-PCR contamination in our samples, which can only be excluded by the use of appropriate controls and procedures, as outlined above. However, we used genomic PCR to amplify the sequence flanking the *EML4-ALK* variant 1 breakpoint in four positive NSCLC samples. Even though a strong amplification product had been obtained from the same DNA templates using primer sets amplifying a control genomic locus of similar size to that of the cases so far reported in literature, no amplification of the *EML4-ALK* variant 1 fusion product was identified, suggesting only a minority of cells carried the *EML4-ALK* gene. These findings concur with Maes et al[2] who reported that, in lymphoid tissues, high level detection of *NPM-ALK* and *ATIC-ALK* fusion transcripts coincided with *ALK* gene rearrangements (as detected by cytogenetics and FISH), whereas low-level detection was not supported by genomic evidence of rearrangements.

In our article,[1] we clearly stated that, unlike observations in ALK+ lymphomas, tumor cells from NSCLC specimens expressed such a low amount of the EML4-ALK fusion protein that immunoprecipitation and immunohistochemistry performed with the commercially available antibodies are unable to detect it. This is in keeping with the observation that the EML4-ALK fusion protein is detectable only using highly sensitive methods, such as mass spectrometry[3] or the intercalated antibody-enhanced polymer (iAEP) method[4] which, unfortunately, are not available in all pathology laboratories and are difficult to standardize. Therefore, the question of how best to detect the EML4-ALK fusion protein remains unanswered.

Issues concerning the frequency, heterogeneity, and tissue specificity of the *EML4-ALK* rearrangement must also be addressed carefully.

Frequency

We recently extended our FISH analysis to 173 surgically resected lung cancer specimens (mainly adenocarcinoma) from an unselected group of Caucasian patients. The incidence of truly positive cases (>50% FISH positive, fusion transcript, and protein positive) was only 0.6% (1/173 cases), which reinforces the results in our artile and is in keeping with Rodig et al's[5] recent report of 1/227 (0.45%) ALK rearranged case in a series of surgically treated Western adenocarcinoma.

Heterogeneity

The heterogeneity of the *EML4-ALK* rearrangement we detected by FISH was confirmed by others in primary tumors

and cell lines[6,7] and is supported by functional studies showing that the magnitude of growth inhibition by siRNA-mediated silencing did not correlate with the number of cells harboring the rearrangement and the lack of growth inhibition in 50% of *EML4-ALK*–positive cell lines. These observations suggest that additional signaling mechanisms independent of ALK may regulate growth and cell proliferation.

Specificity

Claims from Mano's group that the *EML4-ALK* product is specific for NSCLC is contradicted by our findings in normal tissues[1,8] and by a recent study from Lin E. et al,[6] who found *EML4-ALK* fusions in breast (2.4%) and colorectal (2.4%) cancer, in addition to NSCLC.

Finally, we wonder whether it is really appropriate to compare treatments such as ALK inhibitors in NSCLC with imatinib mesylate and gefinitinib/erlotinib in other human neoplasms. In fact: i) the role of EML4-ALK in NSCLC is not as well established as that of BCR/ABL in chronic myeloid leukemia (CML); ii) NSCLC responses to ALK inhibitors[9] are not as remarkable as the CML response to imatinib mesylate; and iii) patients with NSCLC were treated with a multikinase, c-MET and ALK, inhibitor.[9] Considering that about 20% of NSCLC have MET amplification and overexpression and that MET rearrangements are homogeneous in lung cancer,[10] it may be possible that responses to the multikinase inhibitor may be related to other coexisting oncogenic events, independently of ALK.

In conclusion, although we fully acknowledge the importance of Soda et al's discovery,[11] we believe that additional studies are required to elucidate the concurrent genetic events and cellular settings necessary for *EML4-ALK* to exert an oncogenic function and to better define the role of *EML4-ALK* in diagnosis and targeted therapy of NSCLC.

Brunangelo Falini
Maria Paola Martelli
Stefano A. Pileri
Gabriella Sozzi
Patrizia Gasparini

Institute of Hematology, University of Perugia, Perugia, Italy
The Units of Surgical Pathology and Hematopathology,
S. Orsola Hospital, University of Bologna, Bologna, Italy
Fondazione IRCCS, Istituto Nazionale dei Tumori, Milan, Italy

References

1. Martelli MP, Sozzi G, Hernandez L, Pettirossi V, Navarro A, Conte D, Gasparini P, Perrone F, Modena P, Pastorino U, Carbone A, Fabbri A, Sidoni A, Nakamura S, Gambacorta M, Fernandez PL, Ramirez J, Chan JK, Grigioni WF, Campo E, Pileri SA, Falini B: EML4-ALK rearrangement in non-small cell lung cancer and non-tumor lung tissues. Am J Pathol 2009, 174:661–670
2. Maes B, Vanhentenrijk V, Wlodarska I, Cools J, Peeters B, Marynen P, de Wolf-Peeters C: The NPM-ALK and the ATIC-ALK fusion genes can be detected in non-neoplastic cells. Am J Pathol 2001, 158: 2185–2193
3. Rikova K, Guo A, Zeng Q, Possemato A, Yu J, Haack H, Nardone J, Lee K, Reeves C, Li Y, Hu Y, Tan Z, Stokes M, Sullivan L, Mitchell J, Wetzel R, Macneill J, Ren JM, Yuan J, Bakalarski CE, Villen J, Kornhauser JM, Smith B, Li D, Zhou X, Gygi SP, Gu TL, Polakiewicz RD, Rush J, Comb MJ: Global survey of phosphotyrosine signaling identifies oncogenic kinases in lung cancer. Cell 2007, 131:1190–1203
4. Takeuchi K, Choi YL, Togashi Y, Soda M, Hatano S, Inamura K, Takada S, Ueno T, Yamashita Y, Satoh Y, Okumura S, Nakagawa K, Ishikawa Y, Mano H: KIF5B-ALK, a novel fusion oncokinase identified by an immunohistochemistry-based diagnostic system for ALK-positive lung cancer. Clin Cancer Res 2009, 15:3143–3149
5. Rodig SJ, Mino-Kenudson M, Dacic S, Yeap BY, Shaw A, Barletta JA, Stubbs H, Law K, Lindeman N, Mark E, Janne PA, Lynch T, Johnson BE, Iafrate AJ, Chirieac LR: Unique clinicopathologic features characterize ALK-rearranged lung adenocarcinoma in the western population. Clin Cancer Res 2009, 15:5216–5223
6. Lin E, Li L, Guan Y, Soriano R, Rivers CS, Mohan S, Pandita A, Tang J, Modrusan Z: Exon array profiling detects EML4-ALK fusion in breast, colorectal, and non-small cell lung cancers. Mol Cancer Res 2009, 7:1466–1476
7. Perner S, Wagner PL, Demichelis F, Mehra R, Lafargue CJ, Moss BJ, Arbogast S, Soltermann A, Weder W, Giordano TJ, Beer DG, Rickman DS, Chinnaiyan AM, Moch H, Rubin MA: EML4-ALK fusion lung cancer: a rare acquired event. Neoplasia 2008, 10:298–302
8. Sozzi G, Martelli MP, Conte D, Modena P, Pettirossi V, Pileri SA, Falini B: The EML4-ALK transcript but not the fusion protein can be expressed in reactive and neoplastic lymphoid tissues. Haematologica 2009, 94:1307–1311
9. Kwak E, Camidge D, Clark J, Shapiro G, Maki R, Ratain M, Solomon B, Bang Y, Ou S, Salgia R: Clinical acitvity observed in a phase I dose escalation trial of an oral c-met and ALK inhibitor, PF-02341066. J Clin Oncol 2009, 27:15s (Suppl, Abstr 3509)
10. Beau-Faller M, Ruppert AM, Voegeli AC, Neuville A, Meyer N, Guerin E, Legrain M, Mennecier B, Wihlm JM, Massard G, Quoix E, Oudet P, Gaub MP: MET gene copy number in non-small cell lung cancer: molecular analysis in a targeted tyrosine kinase inhibitor naive cohort. J Thorac Oncol 2008, 3:331–339
11. Soda M, Choi YL, Enomoto M, Takada S, Yamashita Y, Ishikawa S, Fujiwara S, Watanabe H, Kurashina K, Hatanaka H, Bando M, Ohno S, Ishikawa Y, Aburatani H, Niki T, Sohara Y, Sugiyama Y, Mano H: Identification of the transforming EML4-ALK fusion gene in non-small-cell lung cancer. Nature 2007, 448:561–566

KIF5B-ALK, a Novel Fusion Oncokinase Identified by an Immunohistochemistry-based Diagnostic System for ALK-positive Lung Cancer

Kengo Takeuchi,[1] Young Lim Choi,[3] Yuki Togashi,[1] Manabu Soda,[3] Satoko Hatano,[1] Kentaro Inamura,[1] Shuji Takada,[3] Toshihide Ueno,[3] Yoshihiro Yamashita,[3] Yukitoshi Satoh,[2] Sakae Okumura,[2] Ken Nakagawa,[2] Yuichi Ishikawa,[1] and Hiroyuki Mano[3,4]

Abstract

Purpose: EML4-ALK is a transforming fusion tyrosine kinase, several isoforms of which have been identified in lung cancer. Immunohistochemical detection of EML4-ALK has proved difficult, however, likely as a result of low transcriptional activity conferred by the promoter-enhancer region of *EML4*. The sensitivity of EML4-ALK detection by immunohistochemistry should be increased adequately.

Experimental Design: We developed an intercalated antibody-enhanced polymer (iAEP) method that incorporates an intercalating antibody between the primary antibody to ALK and the dextran polymer-based detection reagents.

Results: Our iAEP method discriminated between tumors positive or negative for *EML4-ALK* in a test set of specimens. Four tumors were also found to be positive for ALK in an archive of lung adenocarcinoma ($n = 130$) and another 4 among fresh cases analyzed in a diagnostic laboratory. These 8 tumors were found to include 1 with *EML4-ALK* variant 1, 1 with variant 2, 3 with variant 3, and 2 with previously unidentified variants (designated variants 6 and 7). Inverse reverse transcription-PCR analysis revealed that the remaining tumor harbored a novel fusion in which intron 24 of *KIF5B* was ligated to intron 19 of *ALK*. Multiplex reverse transcription-PCR analysis of additional archival tumor specimens identified another case of lung adenocarcinoma positive for *KIF5B-ALK*.

Conclusions: The iAEP method should prove suitable for immunohistochemical screening of tumors positive for ALK or ALK fusion proteins among pathologic archives. Coupling of PCR-based detection to the iAEP method should further facilitate the rapid identification of novel ALK fusion genes such as *KIF5B-ALK*.

Gene fusion is a major mechanism of carcinogenesis in hematologic malignancies and sarcomas (1). Identification of the BCR-ABL fusion kinase, which is generated as a result of the balanced chromosome anomaly t(9;22)(q34;q11) in chronic myelogenous leukemia (2), has thus been followed by the discovery of many fusion-type oncogenes (3). In contrast, it has remained unclear whether such translocation-dependent fusion-type oncogenes also play a major role in the pathogenesis of epithelial tumors. Recently, however, almost 50% of prostate cancer cases have been suggested to harbor gene fusions involving ETS transcription factor loci (4), and we have discovered a recurrent chromosome translocation, inv(2)(p21p23), in non-small cell lung cancer (NSCLC) that results in the production of an EML4-ALK fusion-type protein tyrosine kinase (PTK; refs. 5–8).

Forced expression of EML4-ALK in lung epithelial cells induced the rapid development of hundreds of lung cancer nodules in mice, and peroral administration of inhibitors of the PTK activity of EML4-ALK was shown to clear such tumors from the lungs, demonstrating the pivotal role of EML4-ALK in the pathogenesis of NSCLC positive for this fusion kinase (9). This latter observation also supports the clinical application of ALK

Authors' Affiliations: [1]Division of Pathology, The Cancer Institute, Japanese Foundation for Cancer Research and [2]Department of Thoracic Surgical Oncology, Thoracic Center, Cancer Institute Hospital, Japanese Foundation for Cancer Research, Tokyo, Japan; [3]Division of Functional Genomics, Jichi Medical University, Tochigi, Japan; and [4]CREST, Japan Science and Technology Agency, Saitama, Japan

Received 12/15/08; revised 1/23/09; accepted 2/1/09; published OnlineFirst 4/21/09.

Grant support: Supported in part by Grants-in-Aid for Scientific Research from the Ministry of Education, Culture, Sports, Science, and Technology of Japan as well as by grants from the Japan Society for the Promotion of Science; the Ministry of Health, Labor, and Welfare of Japan; the National Institute of Biomedical Innovation of Japan; the Smoking Research Foundation of Japan; and the Vehicle Racing Commemorative Foundation of Japan.

The costs of publication of this article were defrayed in part by the payment of page charges. This article must therefore be hereby marked *advertisement* in accordance with 18 U.S.C. Section 1734 solely to indicate this fact.

Note: Supplementary data for this article are available at Clinical Cancer Research Online (http://clincancerres.aacrjournals.org/).

Current address of Y. Satoh: Department of Thoracic Surgery, Kitasato University School of Medicine, Kanagawa 228-8520, Japan.

Requests for reprints: Kengo Takeuchi, Division of Pathology, The Cancer Institute, Japanese Foundation for Cancer Research, Tokyo 135-8550, Japan. Phone: 81-3-3520-0111; Fax: 81-3-3570-0558; E-mail: kentakeuchi-tky@umin.net.

doi:10.1158/1078-0432.CCR-08-3248

Translational Relevance

Immunohistochemistry (IHC) is a reliable and relatively easy diagnostic tool to detect pathologic proteins in paraffin-embedded tissues. We have recently discovered an oncogenic fusion tyrosine kinase EML4-ALK in ~5% of non-small cell lung cancer cases. In contrast to the sensitive detection of other ALK fusions, such as NPM-ALK in anaplastic large cell lymphoma, however, IHC-mediated identification of EML4-ALK has been difficult, probably owing to the low expression level of the protein. To overcome such limitation, we here developed an intercalated antibody-enhanced polymer (iAEP) method, which is simple, yet provides high sensitivity in the IHC-mediated detection of EML4-ALK. With iAEP, in addition to the faithful detection of all non-small cell lung cancer specimens known to be positive for EML4-ALK, we have further identified specimens carrying novel variants of EML4-ALK or an unknown oncogenic fusion, KIF5B-ALK. Therefore, iAEP would provide a reliable and sensitive means to detect ALK fusions in human cancers.

inhibitors (6, 10) to treat EML4-ALK–positive lung cancer in humans. It should be noted, however, that multiple isoforms of EML4-ALK, generated mainly as a result of diversity in the breakpoint-fusion point within *EML4* (6, 8, 11, 12), have been identified in NSCLC specimens. The accurate diagnosis of *EML4-ALK*–positive tumors will therefore require detection of all in-frame fusions between *EML4* and *ALK* cDNAs, as exemplified by our multiplex reverse transcription– and PCR-based detection system for *EML4-ALK* (8).

Given that, in many pathology laboratories, most specimens submitted for histopathologic diagnosis are stored as formalin-fixed, paraffin-embedded tissue, the DNA or RNA of which may be substantially degraded, it is desirable to develop a suitable and sensitive means to detect EML4-ALK in such samples. An immunohistochemistry-based diagnostic system is one potential approach to such screening. In contrast to the efficient detection of NPM-ALK fusion proteins in anaplastic large cell lymphoma specimens with such an approach (13), however, many researchers have encountered difficulty in detecting ALK fusion proteins in lung tissue by immunohistochemical analysis (14), possibly as a result of weak transcriptional activity of the promoter-enhancer region of *EML4* that drives the expression of *EML4-ALK* compared with that of the *NPM* promoter. We have now attempted to establish a sensitive screening system for ALK fusion protein–positive tumors with an immunohistochemical approach. Furthermore, with such an approach, we unexpectedly discovered a novel *ALK* fusion gene, *KIF5B-ALK*, in NSCLC.

Materials and Methods

Samples. As a test set of samples for the development of sensitive immunohistochemical detection of EML4-ALK, we examined specimens from 11 patients with NSCLC positive for *EML4-ALK* (previously analyzed in ref. 8) and 10 patients with NSCLC negative for the fusion

Table 1. Immunohistochemical staining of EML4-ALK–positive or EML4-ALK–negative NSCLC specimens and quantitation of *ALK* mRNA

Tumor ID	EML4-ALK variant	Staining intensity						*ALK* mRNA level	
		ALK1	ALK1 with iAEP	5A4	5A4 with iAEP	SP8	SP8 with iAEP	5′ region	3′ region
#4808	V1	-	+	-	+	-	+	1.3	57.3
#9034	V1	-	++	+	++	-/+	++	0	83.3
#9968	V1	-	+	-	+	-	+	15.9	150.1
#2374	V2	-	++	-/+	++	-/+	++	1	182.3
#3121	V2	-	++	-/+	++	-/+	++	0	118.6
#4180	V2	-	++	-/+	++	-/+	++	1.4	124.5
#2075	V3	-	++	-/+	++	-/+	++	7	72
#7969	V3	+	+++	++	+++	+	++	3.6	52.7
#9616	V3	-/+	++	+	++	+	++	5.7	33.8
#8398	V4	-	++	-/+	++	-/+	++	0	118.6
#8993	V5	-	++	-/+	++	-/+	++	1.1	61.4
NC #1	NA	-	-	-	-	-	-/+	1	1
NC #2	NA	-	-	-	-	-	-/+	1.2	5.5
NC #3	NA	-	-	-	-	-/+	+	0.9	8.8
NC #4	NA	-	-	-	-/+	-/+	++	4.1	1.4
NC #5	NA	-	-	-	-	-	+	0.6	2.2
NC #6	NA	-	-	-	-	-	+	0.3	1.1
NC #7	NA	-	-	-	-	-/+	+	4.8	2.7
NC #8	NA	-	-	-	-	-	+	1.7	3.8
NC #9	NA	-	-	-	-	-	+	1.5	3.3
NC #10	NA	-	-	-	-/+	-/+	++	2.5	3

NOTE: Tumor specimens of the test cohort were subjected to immunohistochemical staining with the antibody preparations ALK1, 5A4, or SP8 according to the standard protocol or by the iAEP method. Staining intensity is represented as follows: +++, strongly positive; ++, positive; +, weakly but definitely positive; -/+, indeterminate; -, negative. The abundance of ALK mRNA in the specimens was determined by real-time RT-PCR analysis with the primers targeted to the 5′ or 3′ regions, which correspond to the extracellular and intracellular portions, respectively, of ALK; data are normalized relative to the NC (negative control) #1 specimen.
Abbreviation: NA, not applicable.

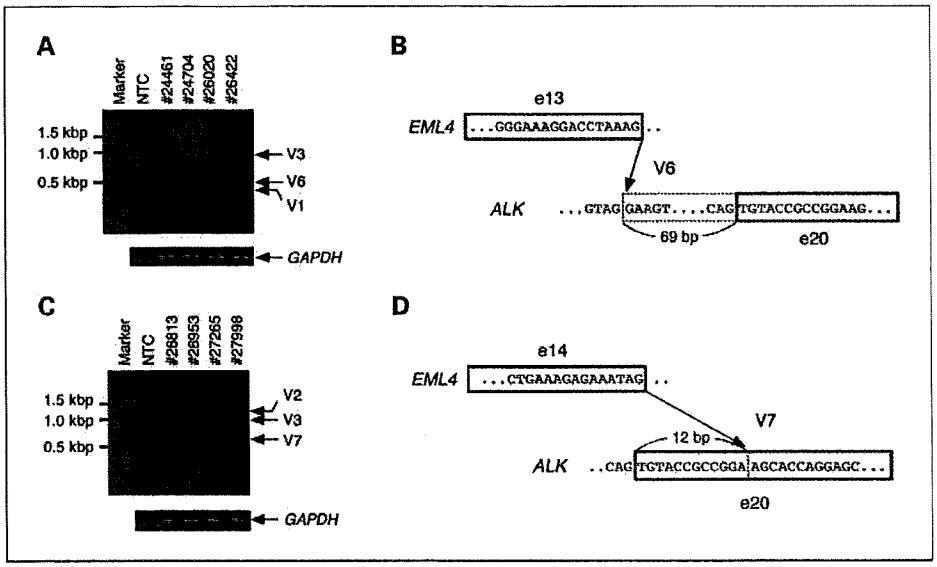

Fig. 1. Identification of novel variants of *EML4-ALK*. *A*, multiplex RT-PCR analysis of all possible in-frame fusions between *EML4* and *ALK* was done with the four specimens of lung adenocarcinoma in the validation cohort that were positive for immunostaining with 5A4 by the iAEP method (*top*). In addition to the detection of *EML4-ALK* variants (*V*)1 and 3 in tumor IDs #24461 and #26422, respectively, a novel PCR product (variant 6) was obtained with tumor ID #26020, whereas no product was obtained with tumor ID #24704. The *GAPDH* cDNA was also amplified as a control for each specimen (*bottom*). Tumor Ids (*top*) and the size of DNA markers (*bottom*; 100-bp ladder) are shown. *Right*, the positions of *EML4-ALK* variants and the PCR product for *GAPDH*. *NTC*, no-template control. *B*, fusion point for *EML4-ALK* variant 6 cDNA. Exon (*e*) 13 of *EML4* is fused to intron 19 of *ALK* at a position 69 bp upstream of exon 20. *C*, multiplex RT-PCR analysis as in *A* for the 4 specimens of lung adenocarcinoma that were identified as positive for immunostaining with 5A4 by the iAEP method in routine diagnostic screening. Tumor IDs #26813 and #26953 were shown to be positive for variant 3 of *EML4-ALK*, whereas #27265 was positive for variant 2. Tumor ID #27988 yielded a PCR product corresponding to a novel variant (variant 7) of *EML4-ALK*. *D*, fusion point of *EML4-ALK* variant 7 cDNA. Exon 14 of *EML4* is fused to nucleotide 13 of exon 20 of *ALK*.

gene. The former cohort comprised 3 cases each for EML4-ALK variants 1, 2, and 3 as well as one case each for variants 4 and 5. As a validation set of samples, we examined specimens from 130 consecutive patients with lung adenocarcinoma, from whom written informed consent was obtained. All specimens were collected with the approval of the ethics committee at the Cancer Institute Hospital (Tokyo, Japan), and the study was approved by the institutional review board of the Japanese Foundation for Cancer Research. Surgically removed cancer specimens were routinely fixed in 20% neutralized formalin and embedded in paraffin. Total RNA was extracted from the corresponding snap-frozen specimens and purified with the use of an RNeasy Mini kit (Qiagen).

Intercalated antibody-enhanced polymer method. Formalin-fixed, paraffin-embedded tissue was sliced at a thickness of 4 μm, and the sections were placed on silane-coated slides. Five antibody preparations specific for the intracellular region of ALK (ALK1 from Dako, 5A4 and SP8 from Abcam, ZAL4 from Zymed, and p80 from Nichirei) were evaluated for immunohistochemical staining according to standard protocols with the use of a dextran polymer reagent (anti-rabbit or anti-mouse immunoglobulin EnVision+DAB system; Dako). On the basis of their reactivity in such experiments, three antibodies (ALK1, 5A4, and SP8) were selected for development of the intercalated antibody-enhanced polymer (iAEP) method as follows. For antigen retrieval, the slides were heated for 40 min at 97°C in Target Retrieval Solution (pH 9.0; Dako). They were then incubated at room temperature first with Protein Block Serum-free Ready-to-Use solution (Dako) for 10 min and then with antibodies to ALK for 30 min. To increase the sensitivity of detection, we included an incubation step of 15 min at room temperature with rabbit polyclonal antibodies to mouse immunoglobulin (Dako) or mouse antibodies to rabbit immunoglobulin (Dako), as appropriate. The immune complexes were then detected with the dextran polymer reagent and an AutoStainer instrument (Dako).

Detection of *EML4-ALK* and *KIF5B-ALK* cDNAs and characterization of their protein products is described in Supplementary Methods.

Results

Development of the iAEP method. A specimen of NPM-ALK–positive anaplastic large cell lymphoma was subjected to immunohistochemical staining with 5 different antibody preparations specific for ALK (ALK1 at a 1:20 dilution, 5A4 at 1:50, SP8 at 1:100, ZAL4 at 1:200, or p80 at 1:100) by the EnVision+DAB polymer method. All antibody preparations stained both the nucleus and cytoplasm of the lymphoma cells, whereas ZAL4 also reacted with normal mesenchymal cells (data not shown). In addition, the staining intensity with p80 was relatively low. We therefore selected ALK1, 5A4, and SP8 for initial development of a detection system for EML4-ALK.

Immunohistochemical analysis of a test set of samples (11 specimens of *EML4-ALK*–positive NSCLC and 10 specimens of *EML4-ALK*–negative NSCLC) with these 3 antibody preparations revealed negative to marginally positive reactivity with EML4-ALK by a conventional staining protocol based on the EnVision+DAB system (Supplementary Fig. S1; Table 1). We therefore incorporated an intercalating antibody before the EnVision+DAB system and applied this iAEP method to the same set of specimens. All three antibody preparations detected EML4-ALK in all *EML4-ALK*–positive cases in the test cohort (Supplementary Fig. S1; Table 1). However, SP8 also reacted with most of the *EML4-ALK*–negative specimens (Supplementary Fig. S2; Table 1), rendering it unsuitable for large-scale screening. Furthermore, a low level of nonspecific background staining of nontumor cells was apparent in all sections stained with ALK1.

We selected ALK1 and 5A4 for examination of a validation set of samples (a consecutive series of 130 lung adenocarcinoma